Broad substrate-specific phosphorylation events are associated with the initial stage of plant cell wall recognition in *Neurospora crassa*

Maria Augusta Crivelente Horta[a], Nils Thieme[a], Yuqian Gao[b], Kristin E. Burnum-Johnson[b], Carrie D. Nicora[b], Marina A. Gritsenko[b], Mary S. Lipton[c], Karthikeyan Mohanraj[d], Leandro José de Assis[e], Liangcai Lin[g], Chaoguang Tian[g], Gerhard H. Braus[k], Katherine A. Borkovich[h], Monika Schmoll[i], Luis F. Larrondo[j], Areejit Samal[d], Gustavo H. Goldman[e,f], J. Philipp Benz[a,f]*

[a] Holzforschung München, TUM School of Life Sciences Weihenstephan, Technical University of Munich, Freising, Germany

[b] Biological Sciences Division, Pacific Northwest National Laboratory, Richland, WA, United States

[c] The Environmental Molecular Sciences Laboratory, Pacific Northwest National Laboratory, Richland, WA

[d] The Institute of Mathematical Sciences (IMSc), Homi Bhabha National Institute (HBNI), Chennai, India

[e] Faculdade de Ciências Farmacêuticas de Ribeirão Preto, Universidade de São Paulo, Ribeirão Preto, Brazil

[f] Institute for Advanced Study, Technical University of Munich, Garching, Germany.

[g] Tianjin Institute of Industrial Biotechnology, Chinese Academy of Sciences, Tianjin, China

[h] Department of Microbiology and Plant Pathology, Institute for Integrative Genome Biology, University of California, Riverside, Riverside, CA, United States

[i] AIT - Austrian Institute of Technology GmbH, Center for Health and Bioresources, Tulln, Austria

[j] Millennium Institute for Integrative Biology (iBio), Departamento de Genética Molecular y Microbiología, Facultad de Ciencias Biológicas, Pontificia Universidad Católica de Chile, Santiago, Chile

[k] Department of Molecular Microbiology and Genetics, Institute of Microbiology and Genetics, University of Goettingen and Goettingen Center for Molecular Biosciences, Goettingen, Germany

***Correspondence:**

J. Philipp Benz

Technical University of Munich – TUM School of Life Sciences Weihenstephan – Holzforschung München

Hans-Carl-von-Carlowitz-Platz 2, D-85354 Freising

Tel.: +49-8161-71-4590

E-mail: benz@hfm.tum.de

Keywords: *Neurospora crassa*, signal transduction, substrate recognition, lignocellulose degradation, fungi, phosphorylation, proteomics

Abstract

Fungal plant cell wall degradation processes are governed by complex regulatory mechanisms, allowing the organisms to adapt their metabolic program with high specificity to the available substrates. While the uptake of representative plant cell wall mono- and disaccharides is known to induce specific transcriptional and translational responses, the processes related to early signal reception and transduction remain largely unkown. A fast and reversible way of signal transmission are post-translational protein modifications, such as phosphorylations, which could initiate rapid adaptations of the fungal metabolism to a new condition. To elucidate how changes in the initial substrate recognition phase of *Neurospora crassa* affect the global phosphorylation pattern, phospho-proteomics was performed after a short (2 minutes) induction period with several plant cell wall-related mono- and disaccharides. The MS/MS-based peptide analysis revealed large-scale substrate-specific protein phosphorylation and de-phosphorylations. Using the proteins identified by MS/MS, a protein-protein-interaction (PPI) network was constructed. The variance in phosphorylation of a large number of kinases, phosphatases and transcription factors indicate the participation of many known signaling pathways, including circadian responses, two-component regulatory systems, MAP kinases as well as the cAMP-dependent and heterotrimeric G-protein pathways. Adenylate cyclase, a key component of the cAMP pathway, was identified as a potential hub for carbon source-specific differential protein interactions. In addition, four phosphorylated F-Box proteins were identified, two of which, Fbx-19 and Fbx-22, were found to be involved in carbon catabolite repression responses. Overall, these results provide unprecedented and detailed insights into a so far less well known stage of the fungal response to environmental cues and allow to better elucidate the molecular mechanisms of sensory perception and signal transduction during plant cell wall degradation.

1. Introduction

Fungi are cell factories with important functions for the bioeconomy since they often exhibit superior metabolic and secretory capabilities compared to bacterial and yeast-based production systems (Meyer et al., 2016). Furthermore, fungi are highly versatile in their ability to adjust their metabolism to diverse substrates. In the case of fungal utilization of complex plant biomass, the specific perception of the individual plant cell wall components is a necessary pre-requisite to adapt enzyme production and intracellular metabolism. These

recognition reactions trigger a sophisticated series of intracellular signaling cascades in order to control and coordinate the cellular response. The fungal perception of plant cell wall polysaccharides in the presence of plant biomass is initiated by starvation-triggered de-repression of a large number of genes, leading to the production of low amounts of scouting enzymes responsible for plant cell wall depolymerization (van Munster et al., 2014). The resulting monomeric and/or small oligomeric soluble sugars are transferred into the cell via membrane-embedded transporters. Then these sugars (or their metabolic derivatives) can function as signaling molecules that activate signal cascades to promote specific metabolic adaptations (see e.g. Glass et al., 2013 and references therein). The recognition signals are responsible for the transcription and translation of specific genes, such as sugar transporters and enzymes necessary to depolymerize and catabolize the corresponding polysaccharide. However, the signaling reactions that occur between the first substrate contact and the gene activation by transcription factors are poorly described, making it difficult to predict good targets for strain engineering.

Reversible modifications in protein phosphorylation mediated by protein kinases or phosphatases represents a mechanism that is frequently employed by eukaryotic cells to transmit environmental cues and initiate signal transduction pathways, such as for transcription factor activation (Whitmarsh and Davis, 2000), cellular localization, protein stability, protein-protein interactions, DNA binding, and enzymatic activity (Breitkreutz et al., 2010; Pawson, 2007). Most cellular processes are in fact regulated by the reversible phosphorylation of proteins on serine (S), threonine (T), and tyrosine residues (Y) (Ficarro et al., 2002; Wart and Unit, 1993), including metabolism, movement, the circadian rhythms and many other (Cohen, 2000; Hurley et al., 2016; Wart and Unit, 1993).

At least 107 serine/threonine protein kinases and more than 30 nucleases and phosphatases are predicted in *Neurospora crassa* (Borkovich et al., 2004; Galagan et al., 2003; Miranda-Saavedra and Barton, 2007; Park et al., 2011), a filamentous ascomycete that has been used as a model system for genetics for many decades and has available a fully sequenced and well-annotated genome (Borkovich et al., 2004). Since *N. crassa* is furthermore a saprotroph growing robustly on complex lignocellulosic material (Seibert et al., 2016; Tian et al., 2009), we used this fungus in the current study to analyze to what extent post-translational protein modifications by phosphorylation are involved in metabolism-related signaling cascades leading to the perception of the individual polysaccharides (cellulose, hemicelluloses and pectin) within complex plant biomass. Little information is available to this end, however regarding the very early time points of the perception event

previous work demostrated the induction of phosphorylation events as early as 2 min after substrate addition (Nguyen et al., 2016; Xiong et al., 2014). Many signaling pathways have already been implicated in the adjustment of fungal metabolism, which involve kinases or phosphatases.

The Mitogen-Activated Protein Kinase (MAP kinase) pathway, for example, represents a prototype of a signal distribution channel with phosphorylation being the major switch. In *N. crassa*, MAP kinases are known to be involved in cell-to-cell communication (Fischer et al., 2018), circadian regulation of cellular processes (Bennett et al., 2013; Lamb et al., 2012), phosphate signaling (Gras et al., 2013) as well as sensing of osmolarity and carbon (Huberman et al., 2017). Phosphorylation/dephosphorylation reactions involved in nutrient-sensing are furthermore central to the cyclic AMP (cAMP) signal transduction pathway (Aichinger et al., 1999; Ficarro et al., 2002; Lengeler et al., 2000). This pathway involves G-protein-coupled receptors (GPCRs), heterotrimeric G proteins, adenylate cyclase, cAMP-dependent protein kinases (PKA) (Lengeler et al., 2000; Lorenz et al., 2000; Xue et al., 1998) and phosphodiesterases. GPCRs are seven-helix transmembrane proteins anchored in the plasma membrane of eukaryotic cells, that are responsible for a diversity of functions, including environmental sensing, metabolism, immunity, growth, and development (Bock et al., 2014; Cabrera et al., 2015; Chini et al., 2013). However, how GPCR-mediated sugar sensing initiates the G-protein signaling reactions and then transduces this signal to the inside of the cell via heterotrimeric G proteins (Tesmer, 2010) is poorly understood. What is known is that cAMP, as the product of the adenylate cyclase, acts as an intracellular secondary messenger (Nauwelaers et al., 2006), regulating a variety of processes including plant cell wall degradation in *Trichoderma, Penicillium, Aspergillus* spp. and *N. crassa* (Dong et al., 1995; Farkas et al., 1990; Schuster et al., 2012) Low amounts of cAMP stimulate cellulase activity, whereas high levels of cAMP repress cellulase formation (Assis et al., 2015). It has been demonstrated in *N. crassa* that one Gα protein, GNA-1, associates with adenylate cyclase (CR-1) and is required for GTP-stimulatable activity (Kays et al., 2000). Some of the morphological aberrations of mutants in this pathway can be complemented by growth in the presence of exogenous cAMP (Kays et al., 2000; Kore-Eda et al., 1991).

Two-component regulatory systems, consisting of proteins with histidine kinase and/or response regulator domains are another system of widespread, ubiquitous signaling pathways in bacteria, slime molds, fungi and plants (Borkovich et al., 2004; Schaller et al., 2011). In fungi, all known histidine kinases are of the hybrid type (HHKs), containing both histidine kinase and response regulator domains within the same protein (Borkovich et al., 2004;

Schaller et al., 2011). A histidine phosphotransfer protein (HPT) receives the phosphate from the response regulator domain of the HHK and in turn transfers this phosphate to an aspartate on a separate, terminal RR protein (Borkovich et al., 2004; Schaller et al., 2011). *N. crassa* possesses 11 HHKs, one HPT, two RRs (Borkovich et al., 2004) and one atypical RR, STK-12 (NCU07378) (Catlett et al., 2003; Park et al., 2011). Mutants lacking *stk-12* have defects in development of aerial hyphae during conidiation (Park et al., 2011). The 11 *N. crassa* HHKs contain additional domains at their N-termini required for normal hyphal growth, resistance to osmotic stress and fungicides, conidial integrity, female fertility (Alex et al., 1996; Schumacher et al., 1997), normal conidiation, pigmentation and perithecial development during the sexual cycle (Barba-ostria et al., 2011; Froehlich et al., 2005). Evidence suggests that the HHK OS-1 (NCU02815) and RRG-1 act upstream of the OS-2/HOG-1 MAP kinase pathway (Jones et al., 2007) and are required for proper control of OS-2 phosphorylation during the circadian rhythm (Vitalini et al., 2007). RRG-2 possesses a Heat Shock transcription Factor (HSF) DNA binding motif and is required for normal sensitivity to oxidative stress (Banno et al., 2007).

Differential phosphorylation of key components in substrate perception was demonstrated for the cellulolytic transcription factors CLR-1, a major cellulase regulator in *N. crassa* (Coradetti et al., 2012, 2013) and XLR-1 (a cellulase/hemicellulase regulator conserved in fungi (Samal et al., 2017) as well as a cellobionic acid transporter, CBT-1, after exposure to cellulose (Xiong et al., 2014). Carbon catabolite repression (CCR) is another central regulatory mechanism involved in substrate perception and metabolic regulation found in a wide range of microbial organisms that ensures the preferential utilization of glucose over less favorable carbon sources (Aro et al., 2005; Vinuselvi et al., 2012) and therefore affects the fungal response to nutrient availability (Fernandez et al., 2012; Nguyen et al., 2016; Bang Wang et al., 2017). Differential phosphorylation of CCR-related proteins after addition of different carbon sources was previously observed in a proteome analysis of *Trichoderma reesei* (Nguyen et al., 2016). In *T. reesei*, the phosphorylation of the transcription factor Cre1, a major mediator for CCR in fungi, at a serine in a conserved stretch within an acidic domain was furthermore found to regulate its DNA binding activity (Cziferszky et al., 2002).

Another protein class known to be involved in metabolic adjustments and CCR are F-Box proteins as part of the SCF complex (Skp, Cullin, F-box containing complex) (Assis et al., 2018; Colabardini et al., 2012; Jonkers and Rep, 2009; Skowyra et al., 1997). This multi-protein E3 ubiquitin ligase complex catalyzes the ubiquitination of proteins destined for the

proteasomal degradation process (Assis et al., 2018; Welchman et al., 2005) and is, therefore, paving the way for new cellular or metabolic states. F-box proteins are found in all eukaryotes and display a large variety of functions. In fungi, they are involved in the control of the cell division cycle, meiosis (Krappmann et al., 2006), mitochondrial connectivity, control of the circadian clock components, fungal development (Kress et al., 2012), virulence (Jöhnk et al., 2016), glucose sensing, as well as the induction of cellulolytic genes (Borkovich et al., 2004; Colabardini et al., 2012). Phosphorylation reactions are a central element of F-box protein-mediated degradation, since F-box target proteins are commonly first phosphorylated before being recognized and ubiquitinated (Jonkers and Rep, 2009). For *A. nidulans*, Fbx23 and Fbx47 were identified as being important for CCR, with the former working in a ubiquitin ligase complex that appears responsible for CreA transcription factor degradation under carbon catabolite-derepressing conditions (Assis et al., 2018). In *T. reesei*, the ubiquitin C-terminal hydrolase CRE2 and the E3 ubiquitin ligase LIM1 play a role in the regulation of cellulase gene expression (Denton and Kelly, 2011; Glass et al., 2013; Gremel et al., 2008). However, the targets of the ubiquitin pathway have not yet been identified, nor is it clear whether the ubiquitinated factor is destined for degradation by the proteasome or if ubiquitination causes a signal-specific activation (Glass et al., 2013; Welchman et al., 2005).

Despite the importance and widespread occurrence of phospho-modifications as laid out above, the identification of sites of protein phosphorylation is still a challenge (Ficarro et al., 2002), hampering the elucidation of its role in global regulatory pathways, such as during substrate perception. Making use of phospho-proteomics analysis by state-of-the-art mass-spectrometry, we aimed to overcome this limitation and determine the phosphorylation patterns during the initial two minutes of contact with new carbon sources. We thus identified a large number of such post-translational modifications in proteins related to the recognition process of plant cell wall compounds by *N. crassa*, such as transcription factors, GPCRs, kinases and F-box proteins. Subsequently, *in silico* methods enabled us to construct putative proteome-wide protein-protein interaction (PPI) maps. Physiological analyses of several components within the cAMP signaling pathway that have clear substrate-dependent phosphorylation changes indicates that they are involved in metabolic adjustments to new carbon-conditions, including CCR.

Overall, this dataset will serve as a benchmark for identification and prediction of phosphorylation reactions during the sensing and signaling of cellulosic carbon sources in filamentous fungi.

2. Research material and methods

2.1 Cell culture and media shift experiments for proteome and phosphoproteome analysis

Flasks with *N. crassa* wild type strain (FGSC #2489) were pre-grown for 16 h on 2% sucrose medium, then washed three times with 1x Vogel's salt solution (no carbon source added) for a total duration of thirty minutes before transferring to their respective carbon source: 1 mM galacturonic acid (D-GalA; Sigma Aldrich) plus 1 mM rhamnose (L-Rha; Sigma Aldrich), referred to as GalAR (D-GalA+L-Rha), 2 mM glucose (D-Glc; Sigma Aldrich), 2 mM xylose (D-Xyl; Sigma Aldrich), 0.5% cellobiose (Cel; Sigma Aldrich) and 1 mM 1,4-ß-D-glucosyl-D-mannose (referred to as Glucomannodextrins or Gm; Megazyme). Samples for global proteome and phosphoproteome were incubated for additional 2 min. No carbon condition (NC) was incubated for 1 h after the medium switch. More details about the experimental methodology for Mass Spectrometry can be found in the Supplementary Material.

2.2. Trypsin digestion

The samples were lysed, reduced, alkylated, and digested by trypsin. Digested samples were desalted using C18 solid phase extraction tubes (Supelco, St.Louis, MO, USA). The resulting peptide samples were concentrated and a bicinchoninic acid (BCA) assay (Thermo Scientific, Waltham, MA, USA) was performed to determine the peptide concentration and samples were diluted with nanopure water for MS analysis. 200 µg peptides aliquots for each sample were dried down for further IMAC enrichment, used for phosphoproteome analysis.

2.3 Phospho-peptide Enrichment by Immobilized Metal Affinity Chromatography (IMAC)

IMAC enrichment of phospho-peptides follows a previously established protocol (Mertins et al., 2018). Peptides were reconstituted in 80 % ACN/0.1% TFA and incubated with Fe^{3+}-NTA agarose bead slurry. Then, the beads containing bound phospho-peptides were washed and desalted using the Stage Tips. After that, the phospho-peptides were eluted from the IMAC beads to the C18 membrane by washing the Stage Tip containing IMAC beads with 70 µl 500 mM phosphate buffer, pH 7.0 and 100 µl 1% FA before being eluted from the C18 membrane with 60 µl 50% ACN/0.1% FA. Eluted phospho-peptides were dried down and stored at -80^{o}C until LC-MS/MS analysis.

2.4. Peptide and phopho-peptide identification by Mass-spectrometry based analysis

The peptide and phospho-peptide samples were both analyzed using a nanoLC system (Waters NanoAcquity LC, Waters Corporation) coupled to a Q Exactive™ Hybrid Quadrupole-Orbitrap™ Mass Spectrometer (Thermo Fisher Scientific) in data dependent mode. All mass spectrometry data were searched using MS-GF+ (Kim et al., 2008; Kim and Pevzner, 2014) to identify peptides by scoring MS/MS spectra against peptides derived from the whole protein sequence database. The MS-GF+ results were filtered based on 1 % false discovery rate (FDR) and less than 5-ppm mass accuracy. Based on spectral count MS data were considered only those peptides that were identified in at least 2 out of 4 experimental replicates with a positive spectrum, independent of the spectral count value. The phospho-peptide results were also searched using AScore algorithm (Gerber et al., 2006) to provide a probability-based score for each identified phospho-peptides. The mass spectrometry proteomics data have been deposited to the ProteomeXchange Consortium via the PRIDE partner repository (Perez-Riverol et al., 2019) with the dataset identifier PXD013964 and 10.6019/PXD013964.

2.5 Protein-Protein Interaction Networks

We constructed a system-wide network of the interactions between proteins found in the global proteome and phospho-proteome of *N. crassa* via prediction of functional interactions between the identified proteins, using the STRING database (Caccia et al., 2013; Szklarczyk et al., 2017). STRING database integrates and reassesses available experimental data from others curated databases, as well as information on structure, domains, function and similarity of proteins to predict functional protein–protein interactions or associations. In the STRING database, the predictions on protein-protein interactions are derived from the following sources: (i) systematic co-expression analysis, (ii) detection of shared selective signals across genomes, (iii) automated text-mining of the scientific literature and (iv) computational transfer of interaction knowledge between organisms based on gene orthology (Szklarczyk et al., 2017). While predicting interactions between *N. crassa* proteins using STRING database, we set the confidence score to be greater than 0.9 and the maximum of additional interactions to 10. Cytoscape was used for the visualization of the PPI network (Shannon et al., 2003). Supplementary Material 1 lists the proteins used to construct the PPI network.

2.6 Cell culture and F-box genes screening

The WT and deletion strains were obtained from the FGSC (http://www. fgsc.net) (McCluskey et al., 2010). The F-box genes were named following *A. nidulans* (Assis et al., 2018; Colabardini et al., 2012): *fbx-9* (*spp-1*, ΔNCU03658, FGSC#21255, Fbx9, AN10061), *fbx-19* (ΔNCU08642, FGSC#15478, Fbx19, AN4510), *fbx-20* (ΔNCU06250, FGSC#15629, Fbx20, AN4535) and *fbx-22* (*cdc4*, ΔNCU05939, FGSC#13190, Fbx22, AN5517). The corresponding deletion strain for *cr-1* (NCU08377) is FGSC#11514.

N. crassa cultures were grown on Vogel's minimal medium (VMM) (Vogel, 1956). Unless noted, 2% (w/v) sucrose was used as a carbon source. Strains were pre-grown on 3 ml VMM slants at 30°C dark for 24 hrs, then at 25°C in constant light for 4–10 days to stimulate conidia production. Conidia were inoculated into liquid media at 1 x 10^6 conidia/ml in individual triplicates and grown at 30°C in constant light and shaking (200 rpm) in 24-deep-well plates. VMM media containing 2% D-Xyl (Sigma Aldrich) as control and 0.2% (w/v) 2-Deoxy-D-glucose (2-DG; Sigma Aldrich) plus 2% D-Xyl were used to test 2- DG influence, evaluated after 4 days. To test allyl alcohol sensitivity, 1% D-Glc +/- 100 mM of allyl alcohol (Sigma Aldrich) were incubated for 2 days.

For xylanase activity assays, the strains were grown in 1% fructose VMM during 24 h at 30°C, then transferred to 2% D-Glc plus 1% D-Xyl VMM, or 1% D-Xyl VMM for 3 days. The xylanase activity was measured in the supernatant using Azo-xylan (from Beechwood; Megazyme) as substrate. Xylanase assays were conducted by mixing 25 µl of culture supernatant with 200 µl of Azo-xylan in 50 µl 1 M sodium acetate, pH 5.0, filling up to a final reaction volume of 400 µl with acetate buffer, and incubated at 37°C for 10 minutes. Reactions were stopped by centrifugation at 7000 x g for 2 min and by addition of 1 ml of precipitation solution (95% v/v ethanol) to the reaction supernatants. The absorbance was measured at 590 nm.

3. Results

3.1. A large number of proteins involved in signaling and perception are variant phosphorylated according brief exposure to new carbon sources

To identify the extent of initial protein phosphorylations upon exposure to new carbon sources, we performed switch experiments, in which sucrose pre-grown *N. crassa* was first starved for 30 minutes and then incubated for two minutes with mono- and disaccharides that are known to act as signaling molecules for plant cell wall-related polysaccharides. This short retention period was deliberately chosen to allow *N. crassa* to take up inducer molecules, but

ensure that the proteome does not have time to significantly change, so that all measured differences are due to post-translational changes as a reaction to nutrient availability and not due to changes in enzyme abundances. A large number of proteins and phospho-peptides were detected by LC-MS/MS analysis in samples from these short-exposure experiments for each induction condition (Supplementary Material 2 – lists the peptides and phospho-peptides identified in different experimental conditions). We want to note that due to the presumed instability of histidine and aspartate phosphorylations during the enrichment strategy, we only searched for phosphorylation of serines (S), threonines (T) and tyrosines (Y) in our approach. We identified 2116 peptides that were phosphorylated equally in all conditions, but also between 207 and 506 phospho-peptides that were found to be phosphorylated specifically in only one condition (Figure 1A). We also studied the representation of the following functional classes among the proteins corresponding to these specific phospho-peptides: transcription factors (TFs), transporters, kinases, metabolism-associated proteins and proteins involved in signal transduction pathways (Figure 1B). The fact that a high number of these signaling-associated protein functions were present in the data sets (Table 1) strongly indicates that carbon sensing and signaling involves protein phosphorylation events as a central component in *N. crassa*.

3.2 Protein-protein interaction networks predict changing signaling pathways in response to different carbon cues

A protein-protein interaction (PPI) network was constructed based on identified proteins in the proteomic and phospho-proteomic experiments, and Figure 2A visualizes this large-scale predicted network of interactions between *N. crassa* proteins present in the cell at the time point of the carbon switch. Thereafter we used the same functional classes (transcription factors, transporters, kinases, metabolism and signal transduction) to analyze the protein distribution across the network. The entire high-resolution network shows that proteins that belong to the same functional class have a tendency to cluster together (Supplementary Material 1). Nevertheless, complex interactions between proteins belonging to different functional classes are also observed in this network, especially in the central position of the network.

To visualize the influence of substrates on this PPI network, the proteins that were identified been phosphorylated under each substrate were highlighted within the network (Figure 2B). Interestingly, it is possible to observe the differences in the profiles of phosphorylation for each substrate induction in Figure 2B. Specifically, the changes in

distribution of highlighted protein nodes on specific induction conditions delineate the differential phosphorylation patterns that occurs in response to each carbon source substrate (Figure 2B).

3.3 A large number of transcription factors exhibit differential phosphorylation upon carbon source perception

An earlier study had estimated the number of TFs in *Neurospora* to be 182 (Borkovich et al., 2004), a number that has been recognized as larger in recent analyses (Carrillo et al., 2017; Weirauch et al., 2014). Thus, we took a conservative list comprising 253 TFs included in the previous studies and inquired for the presence of phospho-sites in the corresponding proteins. One hundred-thirty TFs exhibited one or more phospho-peptides (Supplementary Material 2), with numbers going from one up to several dozens of modified residues per TF. Thus, for example, NIT-2 (NCU09068) exhibited a total of 84 different phospho-peptides, which represents a total of 18 *in vivo* unambiguously modified S and T (with Ascore >13) plus many more for which the localization is less certain. Of these, several are clustered in regions neighboring the GATA-type DNA binding domain (aa positions 742-792) including several that are phosphorylated in different residues. Determining which of the sites (many of which appear conserved in NIT2/AreaA homologues) could be playing regulatory roles, is an interesting question lying ahead.

Another TF exhibiting the second highest number of modifications is NCU10346 (ADA-13). This protein, with a predicted MYB DNA binding domain (PF00249), showed a total number of 43 phospho-peptides, comprising at least 14 unique phosphorylation sites.

Twenty-seven other TFs presented many identified phospho-peptides each, among which were NUC-1 (NCU09315), ASL-1 (NCU01345) and VIB-1 (NCU03725), all transcription factors important in mounting responses to changes in environmental conditions. Thus, for example VIB-1 has been associated with glucose sensing and carbon catabolite repression (Xiong, Sun, et al., 2014), playing a key role under cellulolytic conditions. The different VIB-1 phospho-peptides revealed 10 different phosphorylated residues, one of which also corresponds to a Y (Y107), the latter being modified only upon contact with D-GalA+L-Rha and Glucomannodextrins. T366, located less than 20 aa downstream from the VIB-1 DNA-binding domain, appears modified only in D-Xyl.

CRE-1 (NCU08807), the yeast Mig1 orthologue that plays a key role in carbon catabolite repression, showed six clearly identifiable phosphorylated residues (with Ascore >13) in four different regions of the protein (represented by five different peptides) including

the extreme N- (S6, S11) and C-terminus. While four phospho-sites (S6, S11, S211 and T366) appeared modified in all conditions, some modifications were clearly condition-specific, such as S362 (only on cellobiose, Glucomannodextrins and without carbon source) and S209 (exclusively de-phosphorylated in cellobiose). Which phosphorylations may be modifying CRE-1 activity in *Neurospora* under different culture conditions remain to be determined.

COL-26/BglR (NCU07788) is a TF that has also been involved in glucose sensing/metabolism, regulation of starch degradation as well as the integration of carbon and nitrogen metabolism (Xiong et al., 2017; Xiong, Sun, et al., 2014). Six versions of two different phospho-peptides reveal four unique phosphorylation sites arranged in two pairs (S79/S83 and S674/S676). Interestingly, in glucose and D-GalA+L-Rha, all of the phospho-sites can be observed, while in no carbon condition only S676 was found to be modified.

The cellulase transcription factor CLR-1 (NCU07705) is phosphorylated at two sites, of which S59 phosphorylation was detected under all conditions tested. Phosphorylation of T120, which lies close to the Zn_2-Cys_6 binuclear cluster domain and within the predicted recognition sequence of a cAMP-dependent protein kinase (PKA) phosphorylation site, occurred specifically in the presence of Glucomannodextrins and D-Xyl. This latter phospho-site had already been detected in a previous study (next to S108, which was not identified here; (Xiong et al., 2014) to be more abundant on cellulose vs. no carbon, but found to be dispensable for activation. Of CLR-2 (NCU08042) and XLR-1 (NCU06971), which are also important regulators of cellulase gene transcription in *N. crassa*, no phospho-peptides were detected, peptides of this protein were also not found in the proteomics analysis, indicating a dominating transcriptional kind of regulation, as known for CLR-2 (Coradetti et al., 2012).

Although not a transcription factor, CLR-3 (NCU05846) is still highly relevant for cellulase regulation (Huberman et al., 2017) and was found to be phosphorylated in two regions and three potential sites (Supplementary Material 2). Interestingly, phosphorylation of T713 within a predicted casein kinase II phosphorylation site was specific for the absence of carbon.

3.4 Phosphorylations within two-component regulatory systems

Eight out of the 11 HHKs present in *N. crassa* (Borkovich et al., 2004) were found to be phosphorylated under at least one condition, including DCC-1/NCU00939, NCU01823, NIK-2/NCU01833, NCU02057, OS-1/NCU02815, NCU03164, NCU04615 and NCU07221 (Supplementary Material 2). Of note, the majority of these HHKs (5) were proteins with at least one PAS/PAC domain: DCC-1, NIK-2, NCU02057, NCU03164 and NCU07221. Four

HHKs (DCC-1, NCU01823, NIK-2 and NCU07221) were phosphorylated under all conditions tested. NCU03164 was phosphorylated under every condition except D-Glc and D-Xyl. NCU04615 is unique in only being phosphorylated in the presence of Glucomannodextrins, while this is the only condition under which OS-1 and NCU02057 were not phosphorylated.

HPT-1 (NCU01489) was not phosphorylated under any conditions in this study. RRG-1 (NCU01895) was phosphorylated under all conditions, with three sites in total. RRG-2 (NCU02413) also had two phosphorylation sites and was not phosphorylated during growth on D-Xyl. The atypical RR STK-12 (NCU07378) had 12 regions of phosphorylation and was modified under all conditions. There were two different regions of phosphorylation on protein kinase domain (around S892, T893 and S903) and one in the AGC kinase, C-terminal domain (S1238) of STK-12.

3.5 Carbon specific phosphorylation in the MAP kinase pathways

The MAPKKK SskB/OS-4 (NCU03071), representing the first step in the osmolarity pathway, was found to be phosphorylated at S409 (and potentially S407) in response to D-Glc and Glucomannodextrins, with an additional ambiguous position for cellobiose. Phosphorylation of S1223, S153 and S77 was independent of the applied conditions. Response to cellobiose and no carbon resulted in phosphorylation of T1210, while D-Xyl as well as the D-GalA+L-Rha caused phosphorylation of S123. Interestingly, Glucomannodextrins and D-Xyl elicited phosphorylation of an SSTT-motif (S1343-T1346) within a potential PEST domain (Rechsteiner et al., 1989), suggesting a role for protein degradation in Glucomannodextrins and D-Xyl dependent carbon signaling. Although the AScore for these phosphorylation sites was below 13 (above the threshold of p=0.05; i.e. their precise localization within the peptide is not confirmed) phosphorylation of the respective peptides still indicates a relevance of the PEST domain modification.

In the MAPKK PBS2/OS-5 (NCU00587), condition-independent phosphorylation occurs at serines 219 and 346, while phoshorylation of S482 was only detected in the absence of carbon. The predicted PKC phosphorylation site at S63 is phosphorylated upon recognition of Glucomannodextrins, D-Glc and D-GalA+L-Rha. Phosphorylation of the serines at positions 77 and other sites adjacent to this was found to be condition-dependent for all conditions except no carbon indicating that this area may be a hot spot for post-translational regulation of carbon response in this kinase. HOG1/OS-2 (NCU07024), the MAP kinase of the osmolarity pathway, showed only two phosphorylated sites, one being a tyrosine. For Y173,

phosphorylation was found under all conditions tested. However, phosphorylation of the adjacent T171 obviously required recognition of a carbon source, as no phosphorylated peptide was detected in the absence of carbon.

For NRC-1 (NCU06182), the MAPKKK of the pheromone response pathway, several phospho-peptides were detected. Six phosphorylated amino acids reside within predicted casein kinase phosphorylation sites and one in a PKC phosphorylation site. The serines at positions 49 and 558 were phosphorylated under all conditions tested. The predicted PKC phosphorylation site at S189 appears to be starvation-specific (no carbon) and T872 phosphorylation was only detected on cellobiose. In contrast to the osmolarity pathway, specific phosphorylations were also detected for D-GalA+L-Rha in combination with other carbon sources for NRC-1. In case of the MAPKK MEK-2 (NCU04612), we found phospho-peptides supporting the presence of both protein variants, with phosphorylation of T490 of variant 2 being present under all conditions tested. Despite detection of several phosphorylated sites, only few carbon-specific ones were found: while D-Xyl specifically elicited phosphorylation of S212, which is close to the active site, the serine at position 351 became phosphorylated upon sensing of D-Xyl, D-Glc and D-GalA+L-Rha. The MAP kinase of the pheromone response pathway, MAK-2 (NCU02393), only showed two phosphorylation sites, of which the tyrosine at position 182 was phosphorylated under all conditions tested. However, the adjacent T180 was phosphorylated only in the presence of D-Xyl and D-Glc.

In the cell integrity pathway, the MAPKKK MIK-1 (NCU02234) was found to be broadly phosphorylated under different conditions with up to 27 detected different phospho-peptides with 13 variant residues, albeit some have uncertain localization scores within peptides. In many cases, phosphorylation was not condition-dependent, but both for D-Glc (with S1215, a putative PKC site and S864, a putative casein kinase II site) and D-Xyl (with S1460, a putative cAMP-dependent site) specific sites were obvious. Phosphorylation of S450 was specific to the absence of carbon. Additionally, the region between S477 and S487 appeared to be strongly phosphorylated upon detection of carbon and may hence be a hotspot for carbon dependent regulation. Interestingly, this region overlaps with a poor PEST motif (Rechsteiner and Rogers, 1996), which hints at the involvement of protein degradation of MEK-1 (NCU06419) in regulation. Similarly, the region between amino acids 758 and 762 contains up to four phosphorylated sites specific for different conditions except “no carbon” and may as well represent such a hotspot.

In the MAPKK MEK-1, phospho-peptides were detected for different conditions, suggesting carbon-dependent phosphorylations also for this protein. Additionally, specific

phosphorylations were detected for Glucomannodextrins on amino acids T92, S135, S139 and S184. The clustered serines at positions S130, S135 and S139 were phosphorylated in different combinations in various conditions and could thus represent an important area for carbon sensing. As also this region overlaps with a potential PEST motif, a contribution of protein stability or degradation in carbon sensing is further supported.

Phosphorylation of the MAP kinase MAK-1 (NCU09842) was found to occur on up to five sites, two of which being tyrosines. Thereby, phosphorylation of Y189 occured independently of the conditions tested, while Y185 was only phosphorylated in response to D-Glc (and potentially D-Xyl and Glucomannodextrins, but with low AScores). T187 became phosphorylated in response to plant cell wall-related carbon sources, but not in the absence of carbon.

3.6 Serine/threonine protein kinases are variably phosphorylated under different carbon conditions

Previous studies showed that there are 107 serine/threonine protein kinases in the *N. crassa* genome. According to our results, seventy-three out of the 107 serine/threonine protein kinases were found to be phosphorylated under at least one condition. It is worth noting that HAT-2 (NCU02556) is unique in only being phosphorylated in presence of cellobiose, implying that this modification may be important for cellulose utilization. Furthermore, STK-13 (NCU00108) and STK-47 (NCU06685) were only phosphorylated in response to Glucomannodextrins and D-GalA+L-Rha, respectively. Besides that, STK-39 (NCU06230) appears modified only in starvation condition.

In eukaryotes, protein kinase A (PKA) and the phosphatidylinositol 3-kinase TOR (NCU05608) are two major kinases involved in regulation of cell growth in response to nutritional signals. Yak1 and Sch9 are two downstream targets of these kinase cascades (Lv et al., 2015). Recent investigation showed that TrSch9 and TrYak1 play important roles in cellulase biosythesis in *T. reesei* (Lv et al., 2015). Our results demonstrated that STK-10 (NCU03200), the TrSch9 orthologue in *N. crassa*, exhibited the highest number of modifications upon recognition of cellobiose. This protein showed a total of 12 phosphorylated phospho-peptides (in 62 variants), which represents 22 *in vivo* unambiguously modified S, T and Y, suggesting that these sites may be playing regulatory roles. Similarly, PRK-2/YAK1 (NCU07872), the homolog of *T. reesei* TrYak1, showed 13 distinguishable phosphorylated residues (23 variants), represented in 12 different phospho-peptides under cellobiose condition. Thus, determining the function of these phosphorylation

sites will be a worthwhile target for an increased scientific understanding of cellulase gene expression in filamentous fungi.

There are two catalytic subunits of PKA, namely PKAc-1 (NCU06240) and PKAc-2 (NCU00682), in *N. crassa*. Previous studies showed that PKAc-1 works as the major PKA in *N. crassa*, while deletion of *pkac-2* does not affect fungal morphology, suggesting that these two isoforms may play distinct roles (Banno et al., 2005). According to our results, PKAc-1 was found to be phosphorylated under all tested conditions, while PKAc-2 was phosphorylated only in the presence of D-Glc and cellobiose (for more details, see section 3.11.1).

3.7 Variances in phosphorylation of the G-protein-mediated signaling components

We analyzed the six G-protein subunits (Gα proteins GNA-1/NCU06493, GNA-2/NCU06729, GNA-3/NCU05206; Gβ proteins GNB-1/NCU00440 and CPC-2/NCU05810 and Gγ subunit GNG-1/NCU00041) (Muller et al., 1995; Yang et al., 2002), prosducin and 43 GPCRs, looking for phospho-sites in our dataset (Supplementary Material 2). Of the six G-proteins, only the Gβ subunits GNB-1 and CPC-2 (RACK1 homolog) were phosphorylated. GNB-1 was phosphorylated under all conditions in its extreme N-terminus, while S157 of CPC-2 was found to be phosphorylated only with Glucomannodextrins or without any carbon source.

The phosducin like-protein PhLP1 (NCU00441), which acts as a co-chaperone for β and γ subunits (Willardson and Tracy, 2012) is phosphorylated at S120 and S129 independent of the carbon source. The serines at position 41 and 47 are specifically phoshorylated in presence of Glucomannodextrins.

We furthermore detected 33 distinctive phospho-peptides for 10 GPCRs. This set contains NCU03238 (GPR-9), NCU03253 (GPR-8), NCU04106 (GPR-17), NCU04931 (GPR-18), NCU04987 (GPR-10), NCU06987 (GPR-14), NCU08718 (GPR-35), NCU09195 (GPR-6), NCU09201 (GPR-37) and NCU09427 (GPR-3). Of interest, four of these (GPR-17, 18, 35 and 37) are Pth11-related GPCRs, a large class previously implicated in sensing/degradation of cellulose in *N. crassa* (15). GPR-17 and GPR-35 were phosphorylated under all conditions, with an extra phospho-peptide observed only in the presence of D-Xyl for GPR-17 and during starvation (no carbon source) for GPR-35. GPR-9 was phosphorylated in D-Glc, D-GalA+L-Rha and D-Xyl. GPR-18 was phosphorylated in the presence of D-GalA+L-Rha, cellobiose and Glucomannodextrins, but not D-Glc or starvation, suggesting that this GPCR is phosphorylated only during growth on plant cell wall substrates. Results

552 from RNAseq analysis showed that *gpr-18* is also among the most highly expressed of the
553 Pth11-class GPCRs during growth on avicel (Cabrera et al., 2015).

554 The 10 GPCRs were variously phosphorylated in three different regions of the
555 proteins. GPR-3, GPR-8, GPR-14, GPR-17, GPR-18, GPR-35 and GPR-37 are
556 phosphorylated on residues in the intracellular C-terminal region. The mPR-Like/PAQR
557 GPCRs GPR-9 and GPR-10 are phosphorylated on the first extracellular domain, while Stm1-
558 like GPR-6 is phosphorylated in the large second intracellular loop region.

559

560 ### 3.8 Signaling crosstalk between carbon sensing and components of light response and
561 circadian rhythmicity

562 Even though *Neurospora* was grown under constant light conditions for the present study, the
563 data reveal abundant phosphorylations present in clock components. Crosstalk between gene
564 regulation in response to different nutritional conditions and the light response pathway is
565 extensive (Schmoll, 2018; Stappler et al., 2017) and was also shown in *N. crassa* (Sancar et
566 al., 2012; Schmoll et al., 2012). FREQUENCY (FRQ; NCU02265) is a key component of the
567 *Neurospora* circadian clock, allowing precise daily control of several processes, including
568 metabolism (Hurley et al., 2016; Montenegro-Montero et al., 2015). Under day-night regimes,
569 FRQ is known to be subjected to extensive phosphorylations (> 75 unambiguous S/T sites)
570 throughout its daily cycle, many of which are key in determining the proper pace of the clock
571 (Baker et al., 2009; Larrondo et al., 2015; Tang et al., 2009). Herein, we have confirmed the
572 phosphorylated status of 12 of these residues (seven with AScores >13), while identifying at
573 least one additional site (T289). Out of the known sites, many appear to be phosphorylated
574 under many conditions, while others appear to be modified only upon certain media
575 transitions (Supplementary Material 2). Interestingly, the new *in vivo* determined phospho-site
576 appears to be modified only under D-Glc. However, since we did not control tightly for
577 sampling under identical time-of-day conditions, some of the observed changes might have
578 been affected by the clock. Nevertheless, most of the sites observed in FRQ in this study have
579 been shown to be *in vitro* substrates for CKI or/and CKII activity, such as S28, S145, T289,
580 S462, S683, S685, and S950 (Tang et al., 2009).

581 Two other essential clock components, and also key actors in light-responses, are the
582 transcription factors WC-1 (NCU02356) and WC-2 (NCU00902), which also impact
583 regulation of plant cell wall degrading enzymes (Schmoll et al., 2012). WC-1 and WC-2 act
584 as a heterodimer, forming the White Collar Complex (WCC). Our data verify discrete post-
585 translational modifications of WC-2 in S433, a residue shown impact WCC activity and

586 therefore circadian and light-responses (Sancar et al., 2009). Indeed, recently S433 was shown
587 to be part of a P-cluster in WC-2 required for properly closing the circadian feedback loop
588 (Wang et al., 2019). In the case of WC-1, three different regions were found to be
589 phosphorylated, with one region (S1005-S1015) displaying multiple phosphorylations,
590 particularly in D-Glc condition. These sites are located few residues distal from other
591 phosphorylatable residues known to modulate circadian function of WC-1 (He et al., 2005;
592 Wang et al., 2015; Wang et al., 2019) Some of the sites in WC-1 were recently shown to be
593 phosporylable *in vitro* by CDK-1 (S831) or MAPK (S831 and S1015), without the need of a
594 priming phosphorylation events (Wang et al., 2019). Interestingly, no phospho-peptides were
595 detected for the LOV/PAS domain protein VVD (NCU03967) (Schafmeier and Diernfellner,
596 2011) which is involved in photoadaptation, despite the presence of several predicted
597 phosphorylation sites and detection of the protein under all tested conditions. Finally, FRH
598 (FRQ-interacting RNA helicase; NCU03363) is another key core-clock component, which *in*
599 *vivo* studies have shown to display only one phosphorylation site (S21). Herein, we observed
600 such phosphorylation in all analysed conditions.

601 The transcription factor SUB-1 (NCU01154) is predominantly known for its function
602 in development in diverse fungi (Bazafkan et al., 2017; Colot et al., 2006), but has been
603 shown to be connected to regulation of light response and chromatin remodelling by the white
604 collar complex (Chen et al., 2009; Sancar et al., 2015). In SUB-1, we detected one
605 unambiguous cellobiose-specific phosphorylation site (S381). S247 was phosphorylated under
606 all conditions tested, while S143 was phosphorylated except upon recognition of cellobiose
607 and in the absence of carbon, suggesting a starvation-triggered switch.

608 Also for VE-1 (Velvet; NCU01731), functions in development and secondary
609 metabolism are best known (Bayram et al., 2008; Bayram and Braus, 2011), although this
610 regulator also impacts plant cell wall degradation and light response (Aghcheh et al., 2014;
611 Bayram and Braus, 2011). For VE-1 we detected one constant phospho-modification (S455)
612 and two regions with potentially carbon sensing-relevant phosphorylations, one from T114 to
613 S119, which overlaps with a poor PEST domain and a second one from T262 to T267.
614 Interestingly, these regions contain two cellobiose-specific phosphorylations (T114 and T267,
615 the latter with an Ascore only slightly below our threshold of 13.

616 The finding of clear condition-dependent phosphorylation patterns for both the
617 photoreceptors and their regulators, such as SUB-1 or the casein kinases (see below) adds
618 further support to the crosstalk between the reaction to carbon sources in the environment and
619 sensing of light as well as circadian rhythmicity.

3.9 Phosphorylation of casein kinases

In *N. crassa*, casein kinases are mainly known for their function in the circadian clock (see above) with important impact on FRQ phosphorylation and stability (Diernfellner and Schafmeier, 2011), and are also know in other fungi (Al Quobaili and Montenarh, 2012; Apostolaki et al., 2012). *N. crassa* has one casein kinase II catalytic subunit and two casein kinase regulatory subunit as well as one casein kinase I (Borkovich et al., 2004).

The casein kinase II catalytic subunit alpha (CKA; NCU03124) did not display any detectable phosphorylation. In the casein kinase II regulatory subunit beta-1 (CKB1; NCU05485) however, S291 was found phosphorylated under all conditions tested, while S78, S101, S105, S106 and S223 show carbon-dependent phosphorylation specific to certain carbon sources (S101 and S105 for example to cellobiose and no carbon conditions). For the second casein kinase regulatory beta subunit (CKB2; NCU02754), we could not find any phosphorylated peptides, although the protein was detected under all tested conditions. The C-terminus of casein kinase I (CK-1A; NCU00685) on the other hand is phosphorylated at S313 and S320 (and potentially S312; low Ascore) independent of the condition tested, while S340 (and potentially S338; low Ascore) show carbon-specific phoshporylations including the absence of a carbon source.

3.10 Differential phosphorylation of F-Box proteins indicate that these modifications are necessary for correct protein turnover and metabolic adjustments

The genome of *N. crassa* is predicted to encode for 42 F-Box proteins. For 16 of these, we were able to detect phospho-peptides under at least one condition. Since homologs for some of these phosphorylated proteins had been implicated in regulatory functions of D-Glc utilization and CCR in *A. nidulans* (Assis et al., 2018), the respective *N. crassa* deletion strains were tested in more detail. First, we tested the capability of the strains to grow on different carbon sources (Figure 4A). Particularly the deletion strain for Fbx-22 (NCU05939; CDC4) displayed an aberrant growth phenotype, with improved growth, compared to WT, on D-Glc and glucomannan, while displaying reduced growth on arabinan, xylan and pectin. The deletion strain for Fbx-19 (NCU08642) displayed reduced growth on arabinan and pectin.

To test for a potential role in CCR, we next evaluated the resistance of WT and the mutants to 2-deoxy-glucose (2-DG) and allyl alcohol (AA) (Figure 4B). 2-DG is a non-metabolizable analogue of D-Glc that is often used to indicate impaired glucose repression in filamentous fungi (Allen et al., 1989; Assis et al., 2018; Xiong, Sun, et al., 2014). When

functional, 2-DG is phosphorylated and activates CCR, resulting in the inability of the strain to grow on alternative carbon sources. When mutant strains are impaired in CCR, however, they become resistant to 2-DG. Of the four tested strains, the Δ*fbx-22* mutant showed some 2-DG resistance when 2% D-Xyl was used as an alternative carbon source in the presence of 2-DG (Figure 4B). AA is also used for assessing CCR, as reported for *M. oryzae* (Fernandez et al., 2012) and *A. nidulans* (Assis et al., 2018; Colabardini et al., 2012). When CCR is impaired, alcohol dehydrogenases are expressed despite the presence of D-Glc and will convert AA into the toxic compound acrolein. Thus, strains with impaired CCR exhibit AA sensitivity (Xiong, Sun, et al., 2014). As observed, the mutants Δ*fbx-9* and Δ*fbx-20* were insensitive, similar to WT. The mutants Δ*fbx-19* and Δ*fbx-22*, on the other hand, were sensitive to AA (Figure 4B). These data indicate that F-Box proteins Fbx-19 and particularly Fbx-22 might be involved in the correct signaling of, or adjustment to, conditions of high D-Glc concentrations.

The same AA-sensitivity with reduced growth and conidiation was also described for both homologous genes in *A. nidulans* (Assis et al., 2018). The deletion of these genes in the *A. nidulans* Δ*fbx19* and Δ*fbx22* strains furthermore led to reduced xylanase activity compared to the WT on D-Xyl (Figure 4C). In summary, these phenotypes strongly suggest an at least partially conserved defect of CCR control for Fbx-22 as well as potentially Fbx-19.

3.11 The adenylate cyclase CR-1 is extensively specific phosphorylated and acts as a central hub in the PPI

3.11.1 CR-1 phosphosites identification

In the adenylate cyclase CR-1 (NCU08377), a central component of the cAMP signaling pathway known to be involved in nutritional sensing, we identified 18 unambiguos phosphorylated residues on 31 variant peptides (Figure 3A; Supplementary Material 2). Moreover, we found support for both isoforms of CR-1 with specific phosphorylation in both variants. CR-1 is heavily phosphorylated in both variants under different conditions. Phosphorylation of S67 was specific for cellobiose while T885 was specifically phosphorylated with D-GalA+L-Rha in variant 2. Glucose-specific phosphorylation only occurred in variant 1 at T191 and in the absence of carbon at S161 and S163 (only variant 1). For D-Xyl, specific phosphorylation occurred at T159 in variant 1 and around positions and in a different region at variant 2. Besides the support for two variants of adenylate cyclase by confirmation at the peptide level, these phosphorylation patterns indicate specific functions in

carbon sensing and signaling of individual compounds for both variants. Consequently, *N. crassa* likely distinguishes these carbon sources and triggers specific responses also in terms of alternative splicing and coordinated phosphorylation for their utilization or degradation. Besides CR-1 as the core component, the cAMP pathway further comprises the functionalities of phosphodiesterases, which degrade cAMP in response to environmental signals, and protein kinase A (PKA; see also section 3.6). MCB (NCU01166), the regulatory subunit of PKA, showed phosphorylation in two regions of the N-terminus. In most cases, phosphorylation occured upon sensing of several C-sources or constitutively (e.g. T38, T40). However, phosphorylation of S41 was specific for recognition of D-Xyl and cellobiose. Phosphorylation of the catalytic subunit PKAC-1 (NCU06240) occured predominantly in two areas of the protein: from T19 to T32, containing eight putative phosphorylated sites, and from T377 to Y386. Both regions are overlapping with potential or poor PEST regions. In many cases, multiple parallel phosphorylations occured on several of the tested carbon sources. In contrast to PKAC-1, the second catalytic subunit of protein kinase A, PKAC-2 (NCU00682) showed only two phosphorylated amino acids. Albeit both having low AScores, phosphorylation of Y255 specifically occured in the presence of cellobiose and phosphorylation of T260 was specific for recognition of D-Glc.

The high affinity phosphodiesterase ACON-2 (NCU00478) showed phosphorylation at several sites, in most cases relatively unspecific with respect to the carbon source (particularly S727 and S218). Nevertheless, carbon-specific phosphorylation was observed for Glucomannodextrins at T226 and D-Xyl as well as no carbon at S797, a site that overlaps with a predicted cAMP-dependent phosphorylation site. The low affinity phosphodiesterase PUR-1 (NCU00237) was not detected in the proteome.

3.11.2 CR-1 interaction partners

Within the PPI, CR-1 is predicted to interact with 67 different proteins that form a complex PPI sub-network with a total of 265 connections (Figure 3B). For the visualization of potential carbon source-specific interactions around CR-1, we extracted from the entire network the phosphorylated CR-1-interacting proteins at each condition (Figure 3C). The sub-networks show the different possibilities of phosphorylation cascades that CR-1 might be involved in according to each induction condition. The predicted interactions are in line with the previously mentioned critical function of this gene in the regulation of growth and utilization of carbon sources (Kore-Eda et al., 1991; Lee et al., 1998). This is exemplified by enrichment of specific functional categories within the proteins of the CR-1 sub-networks (Ruepp et al.,

2004) (Supplementary Material 3). For the sub-network from D-Xyl-induction, the most significantly enriched class was protein kinase (30.01.05.01; p-value 1.7E-16), while cAMP/cGMP-mediated signal transduction (30.01.09.07; p-value 7.7E-13) was dominating the Glucomannodextrins-induced subset (next to protein kinases, but with lower p-value: 1.0E-09). For the Cellobiose-induced subset, the top 7 classes were related to activities in the nucleus, such as DNA/RNA synthesis, modification and control (42.10.03, 42.10, 11.02.03, 10.01.09.05, 10.01.09, 11.02, 11.02.03.04, respectively; p-values 3.9E-13, 2.3E-12, 1.5E-11, 1.9E-11, 2.4E-11, 2.9E-11, 7.6E-11), followed by signaling pathways (30.01.09.07, 30.05.01.12.05, 30.05.01.12; p-values 7.7E-11, 3.6E-10, 1.5E-09). In the D-Glc sub-network, nucleus regulation, metal binding and serine/threonine kinase activity were overrepresented (42.10, 42.10.03, 16.17, 30.01.05.01.06; p-values 1.7E-10, 7.4E-10, 7.4E-10, 9.2E-10) plus the protein kinase class, cAMP/cGMP-mediated signal transduction and MAPKKK cascade (30.01.05.01, 30.01.09.07, 30.01.05.01.03; p-values 5.8E-9, 7.8E-9, 9.5E-9, indeed, a connection between MAPK and PKA pathways was described in *A. fumigatus* (Assis et al., 2015). The induction condition that seemed to trigger a high number of different pathways related to signaling and phosphorylation was D-GalA+L-Rha. In this condition, receptor-mediated signaling (30.05.01; p-value 5.5E-14), protein kinase (30.01.05.01; p-value 4.2E-13) and phosphate metabolism (01.04; p-value 3.43E-12) were dominating.

The analysis of the growth phenotype of the respective Δ*cr-1* deletion strain on different substrates demonstrated a substantially decreased capacity to degrade complex substrates (Figure 3D), further corroborating the role of CR-1 as a central hub in the cAMP signaling pathways involved in the sensing and response to environmental conditions.

4 Discussion

Numerous studies have indicated that rapid and reversible protein phosphorylations are involved in many perception pathways of environmental conditions across the tree of life (Cohen, 2000; Hornbeck et al., 2004; Lenoir et al., 2018; Nakagami et al., 2010; Sugiyama et al., 2008; Whitmarsh and Davis, 2000). Also in *N. crassa*, differential phosphorylation during growth on crystalline cellulose, sucrose and carbon-free medium has been described (Xiong et al., 2014). In the present study, we were specifically interested in the initial events of signaling at the onset of perception. For this purpose, we chose to study an extremely early time point (only two minutes after induction), which would be too short for substantial changes on either the transcriptome or proteome levels (Nguyen et al., 2016), but would give us an exclusive insight into rapid post-translational changes. To allow for a fast signal

perception, we utilized soluble mono- and oligosaccharides that are known to act as inducing molecules in fungi, signaling the presence of the respective major plant cell wall polysaccharides: cellobiose for cellulose (Znameroski et al., 2012), D-Xyl for xylan (Sun et al., 2012), D-galacturonic acid and L-rhamnose for pectin (Thieme et al., 2017; Vries et al., 2002), and Glucomannodextrins for mannan (Ogawa et al., 2012). D-Glc and no carbon (starvation) were used as further controls. This extended set of induction conditions allowed us for the first time to identify signaling events that are specific for each of the cues derived from the individual components of a plant cell wall.

To better visualize the complex interplay of phosphorylation reactions, we constructed a protein-protein interaction (PPI) network with all detected proteins, exhibiting 12,066 predicted interactions based on available information gathered from STRING (Szklarczyk et al., 2017). The protein interaction prediction can infer physical and functional protein interactions from the genomic context (Browne et al., 2010; Shoemaker and Panchenko, 2007). PPI networks have already been used to provide insights into protein function and association with complex diseases (Kovács et al., 2019), fungal secretion pathways (Petranovic et al., 2013), identification and association of protein phenotypes (Hu et al., 2011) as well as domain interactions (Browne et al., 2010). Our PPI network represents the first view of possible *N. crassa* protein interactions at the early stage of substrate recognition. While the principal protein classes that putatively participate in the initial stages of substrate recognition (such as kinases, transcription factors, etc.) were found to be clustered across the network, numerous interactions between proteins of different functions are also represented. These interactions include many variances in phosphorylated proteins that can be hypothesized to be part of signaling pathways leading to metabolic adaptations. Detecting the vast changes of phosphorylation patterns across the network in response to different carbon sources strongly indicates that phosphorylation reactions are a central part of the environmental response of *N. crassa* that can be specifically adjusted to the composition of the substrate.

For transcription factors, kinases and other signaling components, such as CR-1, G-proteins and GPCRs, the phosphorylation profile is clearly affected by the substrate composition, providing novel insights into several well-known signaling pathways. For example, the differential phosphorylation of VIB-1, that acts upstream of CRE-1 (Xiong, Sun, et al., 2014), could be a mode of action how this TF is activated or inactivated and thus be involved in the modulation of the activity of CRE-1, potentially supporting the lignocellulolytic response. Further downstream in this regulatory cascade, the cellulase

790 transcription factor CLR-1 shows condition-dependent phosphorylation as well. The
791 regulatory impact of CLR-1 on the transcription factor CLR-2 (Coradetti et al., 2012) could
792 be modulated by this phosphorylation and hence adjusted to the available substrate. As CLR-1
793 binds to its target promotors also under non-inducing conditions (Coradetti et al., 2012; Craig
794 et al., 2015), the observed phosphorylation in presence of Glucomannodextrins and D-Xyl
795 could help to keep CLR-1 de-activated in non-inducing situations.

796 To a large extent, our experiments enable the analysis of the phosphorylation reactions
797 at amino acid resolution (reliably for all phospho-peptides with AScores >13, meaning a p-
798 value for the phospho-site localization < 0.05). Regarding the G-proteins, RACK1-homologs
799 have been demonstrated to function as an alternative Gβ in several fungi and are well-known
800 for their additional role as scaffolding proteins for numerous processes in eukaryotes (Ron et
801 al., 2013; Zhang et al., 2016). In *N. crassa*, the RACK1 homolog *cross-pathway control-2*
802 (CPC-2) is required for proper expression of numerous amino acid biosynthetic enzymes in
803 response to starvation for a single amino acid (Muller et al., 1995). Of interest, one of two
804 residues that are phosphorylated by the WNK8 kinase in plant RACK1 proteins is T162 in the
805 fourth WD40 repeat (J. Chen, 2015; Urano et al., 2015), just three residues away from the *N.*
806 *crassa* phospho-site, which is also found during carbon starvation (no carbon condition).
807 Genetic evidence suggests that phosphorylation of RACK1 on S122 and T162 negatively
808 regulates its functions (Urano et al., 2015).

809 In terms of Gβ, studies in mammals have shown that morphine stimulation leads to
810 phosphorylation and adenylate cyclase activity (Chakrabarti and Gintzler, 2003). Although
811 the causative phospho-site has not been identified, phospho-proteomics studies have identified
812 phosphorylated S residues in the N-terminus at positions 2, 72 and 74 (Chakravorty and
813 Assmann, 2018), analogous to the N-terminal phosphorylation observed in this study. In *S.*
814 *cerevisiae,* the Gβ Ste4p is phosphorylated, but on a T and S residue near the C-terminus of
815 the protein (Chakravorty and Assmann, 2018). This region is not conserved in Gβ subunits
816 from mammals or plants, and yeast mutants lacking both phosphorylation sites have relatively
817 subtle defects in cell polarization during the pheromone response (Chakravorty and Assmann,
818 2018). In the crystal structure of the mammalian Gαβγ heterotrimer, the N-termini of the Gβ
819 and Gγ form interacting α-helices that are important for dimerization (Moreira, 2014). Thus, it
820 is intriguing that Gβ proteins from both *N. crassa* and mammals, but not *S. cerevisiae,* are
821 phosphorylated in this region, perhaps influencing the association of the Gβ and Gγ subunits.

822 Also for the histidine kinase two-component systems, the identified phospho-sites
823 within the domain structure of the proteins provide novel information that might be helpful to

824 better understand their molecular setup. We found that a few of the *N. crassa* HHKs had at
825 least one S/T phosphorylation site within a conserved motif in the protein. S/T
826 phosphorylation of a plant HHK has been demonstrated for the cytokinin receptor AHK2 in
827 *Arabidopsis thaliana* (Dautel et al., 2016; Nakagami et al., 2010; Sugiyama et al., 2008). One
828 of these studies found that T4, S596 and T740 were phosphorylated, the latter two residues
829 within the HK domain of AHK2 (Dautel et al., 2016). In *N. crassa*, two of the seven detected
830 phospho-sites in DCC-1 (NCU00939) were identified within the RR domain, with S1338 and
831 S1359 being phosphorylated under all conditions. NCU01823 was phosphorylated in different
832 regions with two sites in the Orc1-like AAA ATPase domain, S722 and S723. Regarding
833 NIK-2 (NCU01833), one phospho-peptide was detected at the extreme 3' end of the first
834 PAS/PAC domain being phosphorylated under all conditions. NCU03164 displayed four
835 phosphorylation sites and is the only HHK with a site (S966) in the HK domain, being
836 phosphorylated in presence of D-GalA+L-Rha, cellobiose, Glucomannodextrins and no
837 carbon.

838 With the MAP kinase pathway, we evaluated a prototypical threefold phosphorylation
839 cascade impacting osmosensing, pheromone response and cell wall integrity. According to
840 Huberman et al., 2017, a relevant connection between carbon sensing and osmolarity pathway
841 was described in *N. crassa*. The osmosensing (OS) MAPK pathway has been shown to act as
842 a negative regulator of cellulase production in *N. crassa*, with the suggestion that osmolarity
843 serves as a proxy for soluble sugars (Huberman et al., 2017). The Hog1 MAPK and several
844 upstream components of the osmosensing signaling cascade are also required for normal
845 expression of cellulases in *Trichoderma* (Wang et al., 2018). We found changes in
846 phosphorylation across the whole MAP kinase pathway, with particularly heavy
847 phosphorylation in the MAP KKK proteins. In contrast, MAP kinases HOG1, FUS3 and
848 SLT2 contained only few phosphorylated sites. Carbon source-specific phosphorylation was
849 detected for all the pathways, indicating that carbon sensing involves modification of all three
850 MAP kinase pathways. Moreover, for several regions with increased phosphorylation
851 frequency, we detected overlaps with PEST domains (Rechsteiner et al., 1996). Consequently,
852 not only specific phosphorylation, but also protein degradation is likely to play a role in
853 carbon sensing via the MAP kinase pathways. In many cases phospho-peptides with one
854 phosphorylation or two phosphorylations were detected for MAP kinases, while multiple
855 phosphorylation sites occurred in MAPKK and MAPKKK proteins. Hence, the conditions
856 were selected correctly, i. e. during the process of signal recognition, in which the cascade is

postulated to mediate the phosphorylation through the cascade from the MAPKKK (abundant phoshorylation) to the MAP kinase (moderate phosphorylation).

Another important class of proteins that also seems under regulation by phosphorylation are the F-Box proteins. Normally, F-box proteins are substrate receptors that recruit phosphorylated substrates, whereas phosphorylation of the F-box protein itself (due to lack of substrate) often results in autoubiquitination (by the SCF) and self-desctruction. However, phosphorylation of fungal F-box proteins can also affect other cellular functions, such as localization (Jöhnk et al., 2016). This study reveals specific phosphorylation of Fbx-22 (CDC-4) and a strong phenotype in the respective deletion strain, indicating that this gene has a critical function in CCR regulation that appears partly conserved in *N. crassa* and *A. nidulans*. The visualization of the Fbx-22 interaction network predicts that the protein might interact with two different clusters of proteins depending on the substrate conditions (Supplementary Figure 1). It remains to be determined how these interactions can influence the transcriptional response in the context of CCR regulation, showing a complex coordination of CCR by multiple signals.

The entire network visualization can show the differences in the phosphorylation behavior across the conditions, but cannot give a precise idea about the proteins involved in the interactions. We, therefore, decided to do a detailed analysis of the interactions of CR-1, since this enzyme is essential to the cAMP-dependent protein kinase pathway that is involved in cellulase and xylanase production (Assis et al., 2015). Especially for CR-1, the phosphorylation patterns changed drastically across the conditions. Interestingly, a major “hot spot” of phosphorylation appears to lie between two LRR (leucine-rich repeat) regions (Figure 3A). This motif is present in proteins with diverse functions and provides a versatile structural framework for the formation of protein-protein (Kobe and Deisenhofer, 1995; Kobe and Kajava, 2001) and ligand binding sites (Liu et al., 2017). As the structure of LRR motifs can lead to a conformational flexibility necessary to the protein interaction (Kobe and Deisenhofer, 1995), the phosphorylation in between these regions might also affect the binding properties by influencing the conformational structure of the binding sites. The phosphorylation of Ser/Thr residues between subdomains of LRR-RLK (leucine-rich repeat receptor-like protein kinase) was also previously described as being essential for catalytic activation of some protein kinases (Bojar et al., 2014; Liu et al., 2017).

Similarly intriguing, the identifiable sub-networks of CR-1 were found to have a specific design according to the interacting proteins with condition-specific phosphorylations. Extending the previously described importance of adenylate cyclase in development and

891 growth (Ivey and Hoffman, 2005; Kore-Eda et al., 1991; Nauwelaers et al., 2006), our results
892 therefore indicate that variances in phosphorylated CR-1 can interact with many other
893 proteins and trigger specific phosphorylation cascades, depending on the composition of the
894 medium.
895
896 ## 5. Conclusions
897 The present study reveals fundamental changes in global protein phosphorylation during the
898 initial moments of substrate recognition in *N. crassa*. The identification of protein
899 phosphorylation followed by the prediction of protein-protein interactions allowed us to
900 visualize the condition-specific phospho-protein distribution within the network. Many of the
901 identified phospho-proteins are associated with sensing and signaling functions in the cell and
902 thus appear to be involved in the regulatory networks governing the specific metabolic
903 adaptation to plant cell wall polysaccharide degradation. Our protein-protein-interaction
904 network analysis highlights that these differential patterns might lead to vast alterations in the
905 respective sub-networks, as is the case for the adenylate cyclase CR-1, identified as a central
906 hub with variances in phosphorylation patterns in the tested conditions. In many cases, the
907 analysis provided amino acid level resolution, allowing to make assumptions about carbon
908 source-specific structure-function relationships. Overall, the taken approach can therefore
909 greatly help to identify novel functional interactions related to substrate signaling, and the
910 experimental data can serve as a resource for future efforts to elucidate the underlying
911 molecular mechanisms.
912

Authors' contributions

MACH, NT, CT, LL, AS, and JPB jointly conceived the study, and each designed and supervised substantial parts of it. MACH, NT, YG, KEB, CDN, MAG, MSL, and LJA performed the experiments and acquired the data. All authors helped to analyze and interpret the data. MACH, NT, KAB, MS, LL, LFL, and JPB drafted the manuscript, which was critically revised by LJA, CT, GHB, AS and GHG. All authors read and approved the final manuscript.

Acknowledgements

MACH thanks Prof. Anete Pereira de Souza (UNICAMP, Brazil) and the Coordenação de Aperfeiçoamento de Pessoal de Nível Superior, Computational Biology Program (CAPES Foundation, Brazil) for the post-doctoral fellowship (88881.161048/2017-01). GHG acknowledges support by the Fundação de Amparo a Pesquisa do Estado de São Paulo (FAPESP, Brazil), the Conselho Nacional de Desenvolvimento Científico e Tecnológico (CNPq, Brazil), and the Technical University of Munich – Institute for Advanced Study (TUM-IAS), funded by the German Excellence Initiative. LFL thanks for support by iBio, Iniciativa Científica Milenio (MINECON, Chile), CONICYT/FONDECYT (Chile) and the Howard Hughes Medical Institute (USA).

We are grateful for excellent technical assistance by Petra Arnold and Sabrina Paulus (TUM) and we would like to thank N. Louise Glass (UC Berkeley, LBNL) and Qian Liu (TIB, China) for critical reading of the manuscript and Yuxin Yhang (TUM, Germany) for the assistance with the graphical formatting. We furthermore want to acknowledge the Fungal Genetics Stock Center (FGSC; Manhattan, Kansas, USA) for providing their services and strain collection.

A portion of this research was performed using Environmental Molecular Sciences Laboratory (EMSL), a national scientific user facility sponsored by the DOE's Office of Biological and Environmental Research and located at Pacific Northwest National Laboratory (PNNL). PNNL is a multi-program national laboratory operated by Battelle for the Department of Energy (DOE) under Contract DE-AC05-76RLO 1830.

Competing interests

The authors declare that they have no competing interests.

Funding

JPB: DFG grant # BE 6069/3-1

LFL: CONICYT/FONDECYT 1171151

LJA: 2014 / FAPESP, Brazil Grant numbers 2016/007870-9 and 2017/23624-0.

LL and CT: National Natural Science Foundation of China: 31761133018.

KAB acknowledges NIGMS GM068087 and GM086565 and NIFA Hatch Project #CA-R-PPA-6980-H.

6. References

Aghcheh, R.K., Nemeth, Z., Atanasova, L., Fekete, E., Paholcsek, M., Sandor, E., et al. (2014). The VELVET A Orthologue VEL1 of *Trichoderma reesei* Regulates Fungal Development and Is Essential for Cellulase gene expression. *PloS One*, *9*(11), e112799. https://doi.org/10.1371/journal.pone.0112799

Aichinger, C., Kahmann, R., Feldbrügge, M, Kahmann, R. (1999). The MAP kinase Kpp2 regulates mating and pathogenic development in *Ustilago maydis*. Molecular Microbiology, *34*, 1007–1017.

Al Quobaili, F., Montenarh, M. (2012). CK2 and the regulation of the carbohydrate metabolism. Metabolism,*61*(11),1512–1517. https://doi.org/https://doi.org/10.1016/j.metabol.2012.07.011

Alex, L. A., Borkovich, K. A., Simon, M. I. (1996). Hyphal development in Neurospora crassa : Involvement of a two-component histidine kinase. *Proc. Natl. Acad. Sci.*, *93*(4), 3416–3421.

Allen, K. E., Mcnally, M. T., Lowendorf, H. S., Slayman, C. W., Free, S. J. (1989). Deoxyglucose-Resistant Mutants of *Neurospora crassa* : Isolation , Mapping , and Biochemical Characterization. Journal of Bacteriology, *171*(1), 53–58.

Apostolaki, A., Harispe, L., Calcagno-Pizarelli, A. M., Vangelatos, I., Sophianopoulou, V., Arst Jr, H. N., et al. (2012). *Aspergillus nidulans* CkiA is an essential casein kinase I required for delivery of amino acid transporters to the plasma membrane. Molecular Microbiology, *84*(3), 530–549. https://doi.org/10.1111/j.1365-2958.2012.08042.x

Aro, N., Pakula, T., Penttilä, M. (2005). Transcriptional regulation of plant cell wall degradation by filamentous fungi. FEMS Microbiology Reviews, *29*(4), 719–739.

https://doi.org/10.1016/j.femsre.2004.11.006

Assis, L. J., Ulas, M., Ries, L. N. A., Ramli, N. A. M. El, Sarikaya-Bayram, O., Braus, G. H., at al. (2018). Regulation of *Aspergillus nidulans* CreA-Mediated Catabolite Repression by the F-Box Proteins Fbx23 and Fbx47. *mBio*, *9*(3), e00840-18.

Assis, L. J. De, Ries, L. N. A., Savoldi, M., Reis, T. F., Brown, N. A., Goldman, G. H. (2015). *Aspergillus nidulans* protein kinase A plays an important role in cellulase production. Biotechnology for Biofuels, *8*(213), 1–20. https://doi.org/10.1186/s13068-015-0401-1

Baker, C. L., Kettenbach, A. N., Loros, J. J., Gerber, S. A., Dunlap, J. C. (2009). Quantitative Proteomics Reveals a Dynamic Interactome and Phase-Specific Phosphorylation in the *Neurospora* Circadian Clock. Molecular Cell, *34*(3), 354–363. https://doi.org/10.1016/j.molcel.2009.04.023

Banno, S., Noguchi, R., Yamashita, K., Fukumori, F., Kimura, M., Yamaguchi, I., Fujimura, M. (2007). Roles of putative His-to-Asp signaling modules HPT-1 and RRG-2 , on viability and sensitivity to osmotic and oxidative stresses in *Neurospora crassa*. Curr Genet, *51*, 197–208. https://doi.org/10.1007/s00294-006-0116-8

Banno, S., Ochiai, N., Noguchi, R., Kimura, M., Yamaguchi, I., Kanzaki, S., et al. (2005). A catalytic subunit of cyclic AMP-dependent protein kinase, PKAC-1, regulates asexual differentiation in *Neurospora crassa*. Genes & Genetic Systems, *80*(1), 25–34. https://doi.org/10.1266/ggs.80.25

Barba-ostria, C., Lledías, F., Georgellis, D. (2011). The *Neurospora crassa* DCC-1 Protein, a Putative Histidine Kinase, Is Required for Normal Sexual and Asexual Development and Carotenogenesis. Eukaryotic Cell, *10*(12), 1733–1739. https://doi.org/10.1128/EC.05223-11

Bayram, Ö., Braus, G. H. (2011). Coordination of secondary metabolism and development in fungi: the velvet family of regulatory proteins. FEMS, *36*(1), 1–24. https://doi.org/10.1111/j.1574-6976.2011.00285.x

Bayram, Ö., Krappmann, S., Seiler, S., Vogt, N., Braus, G. H. (2008). *Neurospora crassa* ve-1 affects asexual conidiation. Fungal Genetics and Biology, *45*(2), 127–138. https://doi.org/https://doi.org/10.1016/j.fgb.2007.06.001

Bazafkan, H., Beier, S., Stappler, E., Böhmdorfer, S., Oberlerchner, J. T., Sulyok, M., Schmoll, M. (2017). SUB1 has photoreceptor dependent and independent functions in sexual development and secondary metabolism in *Trichoderma reesei*. Molecular Biology, *106*(5), 742–759. https://doi.org/10.1111/mmi.13842

1013 Bennett, L. D., Beremand, P., Thomas, T. L., Bell-Pedersen, D. (2013). Circadian Activation
1014 of the Mitogen-Activated Protein Kinase MAK-1 Facilitates Rhythms in Clock-
1015 Controlled Genes in *Neurospora crassa*. Eukaryotic Cell, *12*(1), 59–69.
1016 https://doi.org/10.1128/EC.00207-12
1017 Bock, A., Kostenis, E., Tränkle, C., Lohse, M. J., Mohr, K. (2014). Pilot the pulse: controlling
1018 the multiplicity of receptor dynamics. Trends in Pharmacological Sciences, *35*(12), 630–
1019 638. https://doi.org/https://doi.org/10.1016/j.tips.2014.10.002
1020 Bojar, D., Martinez, J., Santiago, J., Rybin, V., Bayliss, R., Hothorn, M. (2014). Crystal
1021 structures of the phosphorylated BRI1 kinase domain and implications for
1022 brassinosteroid signal initiation. The Plant Journal, *78*, 31–43.
1023 https://doi.org/10.1111/tpj.12445
1024 Borkovich, K. A., Alex, L. A., Yarden, O., Freitag, M., Turner, G. E., Read, N. D.,et al.
1025 (2004). Lessons from the Genome Sequence of *Neurospora crassa*: Tracing the Path
1026 from Genomic Blueprint to Multicellular Organism. Microbiology and Molecular
1027 Biology reviews, *68*(1), 1–108. https://doi.org/10.1128/MMBR.68.1.1
1028 Breitkreutz, A., Choi, H., Sharom, J. R., Boucher, L., Neduva, V., Larsen, B., et al. (2010). A
1029 Global Protein Kinase and Phosphatase Interaction Network in Yeast. Science, *328*,
1030 1043–1047.
1031 Browne, F., Zheng, H., Wang, H., Azuaje, F. (2010). From Experimental Approaches to
1032 Computational Techniques: A Review on the Prediction of Protein-Protein
1033 Interactions, Advances in Artificial Intelligence, *2010*, 924529, 15.
1034 https://doi.org/10.1155/2010/924529
1035 Cabrera, I. E., Pacentine, I. V, Lim, A., Guerrero, N., Krystofova, S., Li, L.,et al. (2015).
1036 Global Analysis of Predicted G Protein 2 Coupled Receptor Genes in the Filamentous
1037 Fungus , *Neurospora crassa*. *Mol Gen Genet*, *248*(2), 2729–2743.
1038 https://doi.org/10.1534/g3.115.020974
1039 Caccia, D., Dugo, M., Callari, M., Bongarzone, I. (2013). Bioinformatics tools for secretome
1040 analysis. Biochimica et Biophysica Acta, *1834*(11), 2442–2453.
1041 https://doi.org/10.1016/j.bbapap.2013.01.039
1042 Carrillo, A. J., Schacht, P., Cabrera, I. E., Blahut, J., Prudhomme, L., Dietrich, S., et al.
1043 (2017). Functional Profiling of Transcription Factor Genes in *Neurospora crassa*. G3
1044 (Bethesda), *7*(9), 2945–2956. https://doi.org/10.1534/g3.117.043331
1045 Catlett, N. L., Yoder, O. C., Turgeon, B. G. (2003). Whole-Genome Analysis of Two-
1046 Component Signal Transduction Genes in Fungal Pathogens. Eukaryotic Cell, *2*(6),

1151–1161. https://doi.org/10.1128/EC.2.6.1151

Chakrabarti, S., Gintzler, A. R. (2003). Phosphorylation of G is augmented by chronic morphine and enhances G stimulation of adenylyl cyclase activity. Molecular Brain Research, *119*, 144–151. https://doi.org/10.1016/j.molbrainres.2003.09.002

Chakravorty, D., Assmann, S. M. (2018). G protein subunit phosphorylation as a regulatory mechanism in heterotrimeric G protein signaling in mammals, yeast, and plants. Biochemical Journal, *475*, 3331–3357.

Chen, C., Ringelberg, C. S., Gross, R. H., Dunlap, J. C., Loros, J. J. (2009). Genome-wide analysis of light-inducible responses reveals hierarchical light signalling in *Neurospora.* EMBO J., *28*(8), 1029–1042. https://doi.org/10.1038/emboj.2009.54

Chen, J. (2015). Phosphorylation of RACK1 in plants. Plant Signaling & Behavior, *10*(8), e1022013-1.

Chini, B., Parenti, M., Poyner, D. R., Wheatley, M. (2013). G-Protein-Coupled Receptors: from Structural Insights to Functional Mechanisms. Biochemical Society Transactions, *41*(1), 135–136. https://doi.org/10.1042/BST20120344

Cohen, P. (2000). The regulation of protein function by multisite phosphorylation – a 25 year update. Trends in Biochemical Sciences, *25*(12), 596–601. https://doi.org/10.1016/S0968-0004(00)01712-6

Colabardini, A. C., Humanes, A. C., Gouvea, P. F., Savoldi, M., Goldman, M. H. S., Kress, M. R. von Z., et al. (2012). Molecular characterization of the *Aspergillus nidulans fbxA* encoding an F-box protein involved in xylanase induction. Fungal Genetics and Biology, *49*(2), 130–140. https://doi.org/10.1016/j.fgb.2011.11.004

Colot, H. V., Park, G., Turner, G. E., Ringelberg, C., Crew, C. M., Litvinkova, L., et al. Dunlap, J. C. (2006). A high-throughput gene knockout procedure for *Neurospora reveals* functions for multiple transcription factors. PNAS, *103*(44), 10352–10357.

Coradetti, S. T., Craig, J. P., Xiong, Y., Shock, T., Tian, C., Glass, N. L. (2012). Conserved and essential transcription factors for cellulase gene expression in ascomycete fungi. Proc National Acad Sci, *109*(19), 7397–7402. https://doi.org/10.1073/pnas.1200785109

Coradetti, S. T., Xiong, Y., Glass, N. L. (2013). Analysis of a conserved cellulase transcriptional regulator reveals inducer-independent production of cellulolytic enzymes in *Neurospora crassa*. MicrobiologyOpen, *2*(4), 595–609. https://doi.org/10.1002/mbo3.94

Craig, J. P., Coradetti, S. T., Starr, T. L., Glass, N. L. (2015). Direct Target Network of the *Neurospora crassa* Plant Cell Wall. mBio, *6*(5), e01452-15.

https://doi.org/10.1128/mBio.01452-15.Editor

Cziferszky, A., Mach, R. L., Kubicek, C. P. (2002). Phosphorylation positively regulates DNA binding of the carbon catabolite repressor Cre1 of *Hypocrea jecorina (Trichoderma reesei)*. Journal of Biological Chemistry, *277*(17), 14688–14694. https://doi.org/10.1074/jbc.M200744200

Dautel, R., Wu, X. N., Heunemann, M., Schulze, W. X., Harter, K. (2016). The Sensor Histidine Kinases AHK2 and AHK3 Proceed into Multiple Serine / Threonine / Tyrosine Phosphorylation Pathways in *Arabidopsis thaliana*. Mol Plant, *9*(1), 182–186. https://doi.org/10.1016/j.molp.2015.10.002

Denton, J. A., Kelly, J. M. (2011). Disruption of *Trichoderma reesei cre2*, encoding an ubiquitin C-terminal hydrolase, results in increased cellulase activity. BMC *Biotechnology*, *11*, 103. https://doi.org/10.1186/1472-6750-11-103

Diernfellner, A. C. R., Schafmeier, T. (2011). Phosphorylations□: making the *Neurospora crassa* circadian clock tick. Febs Journal, *585*(10), 1461–1466. https://doi.org/10.1016/j.febslet.2011.03.049

Dong, W., Yinbo, Q., Peiji, G. (1995). Regulation of cellulase synthesis in mycelial fungi: Participation of ATP and cyclic AMP. Biotechnology Letters, *17*(6), 593–598. https://doi.org/10.1007/BF00129384

Farkas, V., Gresik, M., Kolarova, N., Sulova, Z., Sestak, S. (1990). Biochemical and physiological changes during photoinduced conidiation and derepression of cellulase synthesis in *Trichoderma*. In Trichoderma reesei cellulases: biochemistry, genetics, physiology and application. (pp. 139–155). Cambridge: Royal Society of Chemistry.

Fernandez, J., Wright, J. D., Hartline, D., Quispe, C. F., Madayiputhiya, N., Wilson, R. A. (2012). Principles of Carbon Catabolite Repression in the Rice Blast Fungus□: Tps1 , Nmr1-3 , and a MATE – Family Pump Regulate Glucose Metabolism during Infection. PLoS Genetics, *8*(5). https://doi.org/10.1371/journal.pgen.1002673

Ficarro, S. B., McCleland, M. L., Stukenberg, P. T., Burke, D. J., Ross, M. M., Shabanowitz, J., et al. (2002). Phosphoproteome analysis by mass spectrometry and its application to *Saccharomyces cerevisiae*. Nature Biotechnology, *20*(3), 301–305. https://doi.org/10.1038/nbt0302-301

Fischer, M. S., Wu, V. W., Lee, J. E., O'Malley, R. C., Glass, N. L. (2018). Regulation of Cell-to-Cell Communication and Cell Wall Integrity by a Network of MAP Kinase Pathways and Transcription Factors in *Neurospora crassa*. Genetics, *209*, 489–506.

Froehlich, A. C., Noh, B., Vierstra, R. D., Loros, J., Dunlap, J. C. (2005). Genetic and

Molecular Analysis of Phytochromes from the Filamentous Fungus *Neurospora crassa*. Eukaryotic Cell, *4*(12), 2140–2152. https://doi.org/10.1128/EC.4.12.2140

Galagan, J., Calvo, S., Borkovich, K., Selker, E., Read, N., Jaffe, D., et al. (2003). The genome sequence of the filamentous fungus *Neurospora crassa*. Nature, *422*(6934), 859–868. https://doi.org/doi: 10.1038/nature01554

Gerber, S. A., Rush, J., Gygi, S. P., Beausoleil, S. A., Ville, J. (2006). A probability-based approach for high-throughput protein phosphorylation analysis and site localization. Nat Biotech, *24*(10), 1285–1292. https://doi.org/10.1038/nbt1240

Glass, N. L., Schmoll, M., Cate, J. H. D., Coradetti, S. (2013). Plant Cell Wall Deconstruction by Ascomycete Fungi. Annual Review of Microbiology, *67*(1), 477–498. https://doi.org/10.1146/annurev-micro-092611-150044

Gras, D. E., Persinoti, G. F., Peres, N. T. A., Martinez-Rossi, N. M., Tahira, A. C., Reis, E. M., et al. (2013). Transcriptional profiling of *Neurospora crassa* Δmak-2 reveals that mitogen-activated protein kinase MAK-2 participates in the phosphate signaling pathway. Fungal Genetics and Biology, *60*, 140–149. https://doi.org/10.1016/j.fgb.2013.05.007

Gremel, G., Dorrer, M., Schmoll, M. (2008). Sulphur metabolism and cellulase gene expression are connected processes in the filamentous fungus *Hypocrea jecorina* (anamorph *Trichoderma reesei*). BMC Microbiology, *8*, 1–18. https://doi.org/10.1186/1471-2180-8-174

He, Q., Shu, H., Cheng, P., Chen, S., Wang, L., Liu, Y. (2005). Light-independent phosphorylation of WHITE COLLAR-1 regulates its function in the *Neurospora* circadian negative feedback loop. The Journal of Biological Chemistry, *280*(17), 17526–17532. https://doi.org/10.1074/jbc.M414010200

Hornbeck, P. V, Chabra, I., Kornhauser, J. M., Skrzypek, E., Zhang, B. (2004). PhosphoSite: A bioinformatics resource dedicated to physiological protein phosphorylation. Proteomics, *4*(6), 1551–1561. https://doi.org/10.1002/pmic.200300772

Hu, L., Huang, T., Liu, X., Cai, Y. (2011). Predicting Protein Phenotypes Based on Protein-Protein Interaction Network. PLoS One, *6*(3), e17668. https://doi.org/10.1371/journal.pone.0017668

Huberman, L. B., Coradetti, S. T., Glass, N. L. (2017). Network of nutrient-sensing pathways and a conserved kinase cascade integrate osmolarity and carbon sensing in *Neurospora crassa*. PNAS, *114*(41), E8665–E8674. https://doi.org/10.1073/pnas.1707713114

Hurley, J. M., Loros, J. J., Dunlap, J. C. (2016). The circadian system as an organizer of

metabolism. Fungal Genet Biol, *90*, 39–43. https://doi.org/10.1016/j.fgb.2015.10.002.The

Ivey, F. D., Hoffman, C. S. (2005). Direct activation of fission yeast adenylate cyclase by the Gpa2 G alpha of the glucose signaling pathway. PNAS, *102*(17), 6180–6113.

Jöhnk, B., Bayram, Ö., Abelmann, A., Heinekamp, T., Mattern, D. J., Brakhage, A. A., et al. (2016). SCF Ubiquitin Ligase F-box Protein Fbx15 Controls Nuclear Co-repressor Localization, Stress Response and Virulence of the Human Pathogen *Aspergillus fumigatus*. PLoS Pathogens, *12*(9), 1–30. https://doi.org/10.1371/journal.ppat.1005899

Jones, C. A., Greer-Phillips, S. E., Borkovich, K. A. (2007). The Response Regulator RRG-1 Functions Upstream of a Mitogen-activated Protein Kinase Pathway Impacting Asexual Development, Female Fertility, Osmotic Stress, and Fungicide Resistance in *Neurospora crassa*. Molecular Biology of the Cell, *18*(June), 2123–2136. https://doi.org/10.1091/mbc.E06

Jonkers, W., Rep, M. (2009). Lessons from fungal F-Box proteins. Eukaryotic Cell, *8*(5), 677–695. https://doi.org/10.1128/EC.00386-08

Kays, A. M., Rowley, P. S., Baasiri, R. A., Borkovich, K. A. (2000). Regulation of Conidiation and Adenylyl Cyclase Levels by the G alpha Protein GNA-3 in *Neurospora crassa*.Molecular and Cellular Biology, *20*(20), 7693–7705.

Kim, S., Gupta, N., Pevzner, P. A. (2008). Spectral probabilities and generating functions of tandem mass spectra: a strike against decoy databases. Journal of Proteome Research, *7*(8), 3354–3363. https://doi.org/10.1021/pr8001244

Kim, S., Pevzner, P. A. (2014). MS-GF+ makes progress towards a universal database search tool for proteomics. Nature Communications, *5*, 5277.

Kobe, B., Deisenhofer, J. (1995). A structural basis of the interactions between leucine-rich repeats and protein ligands. Nature, Letters, *374*, 183–186.

Kobe, B., Kajava, A. V. (2001). The leucine-rich repeat as a protein recognition motif. Current Opinion in Structural Biology, *11*, 725–732.

Kore-Eda, S., Murayama, T., Uno, I. (1991). Isolation and Characterization of the adenylate cyclase structural gene of *Neurospora crassa*. Jpn.J.Gnet., *66*, 317–334.

Kovács, I. A., Luck, K., Spirohn, K., Wang, Y., Pollis, C., Schlabach, S., et al. (2019). Network-based prediction of protein interactions. Nature Communications, *10*(1240), 1–8. https://doi.org/10.1038/s41467-019-09177-y

Krappmann, S., Jung, N., Medic, B., Busch, S., Prade, R. A., Braus, G. H. (2006). The *Aspergillus nidulans* F-box protein GrrA links SCF activity to meiosis. Molecular

Microbiology, *61*(1), 76–88. https://doi.org/10.1111/j.1365-2958.2006.05215.x

Kress, M. R. Z., Harting, R., Bayram, Ö., Christmann, M., Irmer, H., Valerius, O., et al. (2012). The COP9 signalosome counteracts the accumulation of cullin SCF ubiquitin E3 RING ligases during fungal development. Molecular Microbiology, *83*(6), 1162–1177. https://doi.org/10.1111/j.1365-2958.2012.07999.x

Lamb, T. M., Finch, K. E., Bell-Pedersen, D. (2012). The *Neurospora crassa* OS MAPK pathway-activated transcription factor ASL-1 contributes to circadian rhythms in pathway responsive clock-controlled genes. Fungal Genetics and Biology, *49*(2), 180–188. https://doi.org/https://doi.org/10.1016/j.fgb.2011.12.006

Larrondo, L. F., Olivares-Yañez, C., Baker, C. L., Loros, J. J., Dunlap, J. C. (2015). Decoupling circadian clock protein turnover from circadian period determination. Science, *347*(6221). https://doi.org/10.1126/science.1257277

Lee, I. H., Walline, R. G., Plamann, M. (1998). Apolar growth of *Neurospora crassa* leads to increased secretion of extracellular proteins. Molecular Microbiology, *29*(1), 209–218. https://doi.org/10.1046/j.1365-2958.1998.00923.x

Lengeler, K. B., Davidson, R. C., D'souza, C., Harashima, T., Shen, W.-C., Wang, P., et al (2000). Signal Transduction Cascades Regulating Fungal Development and Virulence. Microbiology and Molecular Biology Reviews, *64*(4), 746–785. https://doi.org/10.1128/MMBR.64.4.746-785.2000

Lenoir, M., Ustunel, C., Rajesh, S., Kaur, J., Moreau, D., Gruenberg, J., Overduin, M. (2018). Phosphorylation of conserved phosphoinositide binding pocket regulates sorting nexin membrane targeting. Nature Communications, *9*(1), 993. https://doi.org/10.1038/s41467-018-03370-1

Liu, P., Du, L., Huang, Y., Gao, S., Yu, M. (2017). Origin and diversification of leucine-rich repeat receptor-like protein kinase (LRR-RLK) genes in plants. BMC Evolutionary Biology, *17*(47), 1–16. https://doi.org/10.1186/s12862-017-0891-5

Lorenz, M. C., Pan, X., Harashima, T., Cardenas, M. E., Xue, Y., Hirsch, J. P., Heitman, J. (2000). The G Protein-Coupled Receptor Gpr1 Is a Nutrient Sensor That Regulates Pseudohyphal Differentiation in *Saccharomyces cerevisiae*. Genetics, *154*(2), 609 LP-622.

Lv, X., Zhang, W., Chen, G., Liu, W. (2015). *Trichoderma reesei* Sch9 and Yak1 regulate vegetative growth, conidiation, and stress response and induced cellulase production. Journal of Microbiology, *53*(4), 236–242. https://doi.org/10.1007/s12275-015-4639-x

McCluskey, K., Wiest, A., Plamann, M. (2010). The fungal genetics stock center: A

repository for 50 years of fungal genetics research. Journal of Biosciences, *35*(1), 119–126. https://doi.org/10.1007/s12038-010-0014-6

Mertins, P., Tang, L. C., Krug, K., Clark, D. J., Gritsenko, M. A., Chen, L., et al. (2018). Reproducible workflow for multiplexed deep-scale proteome and phosphoproteome analysis of tumor tissues by liquid chromatography – mass spectrometry. Nature Protocols, *13*, 1632–1661.

Meyer, V., Andersen, M. R., Brakhage, A. A., Braus, G. H., Caddick, M. X., Cairns, T. C., et al. (2016). Current challenges of research on filamentous fungi in relation to human welfare and a sustainable bio-economy: a white paper. Fungal Biology and Biotechnology, *3*(1), 6. https://doi.org/10.1186/s40694-016-0024-8

Miranda-Saavedra, D., Barton, G. J. (2007). Classification and functional annotation of eukaryotic protein kinases. Proteins, *68*, 893–914. https://doi.org/10.1002/prot

Montenegro-Montero, A., Canessa, P., Larrondo, L. F. (2015). Chapter Four - Around the Fungal Clock: Recent Advances in the Molecular Study of Circadian Clocks in *Neurospora* and Other Fungi. In T. Friedmann, J. C. Dunlap,S.F. Goodwin (Eds.) (Vol. 92, pp. 107–184). Academic Press. https://doi.org/https://doi.org/10.1016/bs.adgen.2015.09.003

Moreira, I. S. (2014). Structural features of the G-protein/GPCR interactions. Biochimica et Biophysica Acta, *1840*(1), 16–33. https://doi.org/https://doi.org/10.1016/j.bbagen.2013.08.027

Muller, F., Kruger, D., Sattlegger, E., Hoffmann, B., Ballario, P., Kanaan, M., Barthelmess, I. B. (1995). The *cpc-2* gene of *Neurospora crassa* encodes a protein entirely composed of WD-repeat segments that is involved in general amino acid control and female fertility. *Molecular & General Genetics : MGG*, *248*(2), 162–173.

Nakagami, H., Sugiyama, N., Mochida, K., Daudi, A., Yoshida, Y., Toyoda, T., et al. (2010). Large-Scale Comparative Phosphoproteomics Identifies Conserved Phosphorylation Sites in Plants. Plant Physiol., *153*(6), 1161–1174. https://doi.org/10.1104/pp.110.157347

Nauwelaers, D., Thevelein, J. M., Versele, M., Peeters, T., Louwet, W., Gelade, R. (2006). Kelch-repeat proteins interacting with the G alpha protein Gpa2 bypass adenylate cyclase for direct regulation of protein kinase A in yeast. PNAS, *103*(35), 13034–13039. https://doi.org/10.1073/pnas.0509644103

Nguyen, E. V., Imanishi, S. Y., Haapaniemi, P., Yadav, A., Saloheimo, M., Corthals, G. L., Pakula, T. M. (2016). Quantitative Site-Specific Phosphoproteomics of *Trichoderma*

reesei Signaling Pathways upon Induction of Hydrolytic Enzyme Production. Journal of Proteome Research, *15*(2), 457–467. https://doi.org/10.1021/acs.jproteome.5b00796

Ogawa, M., Kobayashi, T., Koyama, Y. (2012). ManR, a novel Zn(II)2Cys6 transcriptional activator, controls the β-mannan utilization system in *Aspergillus oryzae*. Fungal Genetics and Biology, *49*(12), 987–995. https://doi.org/https://doi.org/10.1016/j.fgb.2012.09.006

Park, G., Servin, J. A., Turner, G. E., Altamirano, L., Colot, H. V, Collopy, P., et al. (2011). Global Analysis of Serine-Threonine Protein Kinase Genes in *Neurospora crassa*. Eukaryotic Cell, *10*(11), 1553–1564. https://doi.org/10.1128/EC.05140-11

Pawson, T. (2007). Dynamic control of signaling by modular adaptor proteins. Current Opinion in Cell Biology, *19*, 112–116. https://doi.org/10.1016/j.ceb.2007.02.013

Perez-Riverol Y., Csordas A., Bai J., Bernal-Llinares M., Hewapathirana S., Kundu D.J., et al. (2019). The PRIDE database and related tools and resources in 2019: improving support for quantification data. Nucleic Acids Res 47(D1):D442-D450.

Petranovic, D., Bordel, S., Nielsen, J., Feizi, A., Tobias, O. (2013). Genome-Scale Modeling of the Protein Secretory Machinery in Yeast. PLos One, *8*(5), e63284. https://doi.org/10.1371/journal.pone.0063284

Rechsteiner, M., Rogers, S. (1996). PEST sequences and regulation by proteolysis. Trends Biochem Sci, *21*(7), 267–271.

Ron, D., Adams, D. R., Baillie, G. S., Long, A., Connor, R. O., Kiely, P. A. (2013). RACK (1) to the future – a historical perspective. Cell Communication and Signaling, *11*(1), 53. https://doi.org/10.1186/1478-811X-11-53

Ruepp, A., Zollner, A., Maier, D., Albermann, K., Hani, J., Mannhaupt, G., et al. (2004). The FunCat , a functional annotation scheme for systematic classification of proteins from whole genomes. Nucleic Acids Research, *32*(18), 5539–5545. https://doi.org/10.1093/nar/gkh894

Samal, A., Craig, J. P., Coradetti, S. T., Benz, J. P., Eddy, J. A., Price, N. D., Glass, N. L. (2017). Network reconstruction and systems analysis of plant cell wall deconstruction by *Neurospora crassa*. Biotechnology for Biofue*ls*, *10*(1), 1–21. https://doi.org/10.1186/s13068-017-0901-2

Sancar, C., Ha, N., Yilmaz, R., Tesorero, R., Fisher, T. (2015). Combinatorial Control of Light Induced Chromatin Remodeling and Gene Activation in *Neurospora*. PLoS Genetics, *11*(3), 1–26. https://doi.org/10.1371/journal.pgen.1005105

Sancar, G., Sancar, C., Brunner, M. (2012). Metabolic compensation of the *Neurospora* clock

by a glucose-dependent feedback of the circadian repressor CSP1 on the core oscillator. Genes Dev, *26*(21), 2435–2442. https://doi.org/10.1101/gad.199547.112

Sancar, G., Sancar, C., Brunner, M., Schafmeier, T. (2009). Activity of the circadian transcription factor White Collar Complex is modulated by phosphorylation of SP-motifs. FEBS Letters, *583*(12), 1833–1840. https://doi.org/10.1016/j.febslet.2009.04.042

Schafmeier, T., Diernfellner, A. C. R. (2011). Light input and processing in the circadian clock of *Neurospora*. FEBS Letters, *585*(10), 1467–1473. https://doi.org/10.1016/j.febslet.2011.03.050

Schaller, G. E., Shiu, S., Armitage, J. P. (2011). Two-Component Systems and Their Co-Option for Eukaryotic Signal Transduction Review. Current Biology, *21*, R320–R330. https://doi.org/10.1016/j.cub.2011.02.045

Schmoll, M. (2018). Regulation of plant cell wall degradation by light in *Trichoderma*. Fungal Biology and Biotechnology, *5*(10), 1–20. https://doi.org/10.1186/s40694-018-0052-7

Schmoll, M., Tian, C., Sun, J., Tisch, D., Glass, N. L. (2012). Unravelling the molecular basis for light modulated cellulase gene expression - the role of photoreceptors in *Neurospora crassa*. BMC Genomics, *13*(127), 1–18. https://doi.org/10.1186/1471-2164-13-127

Schumacher, M. M., Enderlin, C. S., Selitrennikoff, C. P. (1997). The *osmotic*-1 locus of *Neurospora crassa* encodes a putative histidine kinase similar to osmosensors of bacteria and yeast. Current Microbiology, *34*(6), 340–347.

Schuster, A., Tisch, D., Seidl-Seiboth, V., Kubicek, C. P., Schmoll, M. (2012). Roles of protein kinase A and adenylate cyclase in light-modulated cellulase regulation in *Trichoderma reesei*. Applied and Environmental Microbiology, *78*(7), 2168–2178. https://doi.org/10.1128/AEM.06959-11

Seibert, T., Thieme, N., Benz, J. P. (2016). The Renaissance of *Neurospora crassa*: How a Classical Model System is Used for Applied Research. In Gene Expression Systems in Fungi: Advancements and Applications (pp. 59–96). https://doi.org/10.1007/978-3-319-27951-0_3

Shannon, P., Markiel, A., Ozier, O., Baliga, N. S., Wang, J. T., Ramage, D., et al. (2003). Cytoscape□: A Software Environment for Integrated Models of Biomolecular Interaction Networks. Genome Research, 2498–2504. https://doi.org/10.1101/gr.1239303.metabolite

Shoemaker, B. A., Panchenko, A. R. (2007). Protein and Domain Interaction Partners Methods for Predicting Protein Interaction Partners. PLoS Computational Biology, *3*(4),

e43. https://doi.org/10.1371/journal.pcbi.0030043

Skowyra, D., Craig, K. L., Tyers, M., Elledge, S. J., Harper, J. W. (1997). F-Box Proteins Are Receptors that Recruit Phosphorylated Substrates to the SCF Ubiquitin-Ligase Complex. Cell Press, *91*, 209–219.

Stappler, E., Dattenböck, C., Tisch, D., Schmoll, M. (2017). Analysis of Light- and Carbon-Specific Transcriptomes Implicates a Class of G- Protein-Coupled Receptors in Cellulose Sensing. mSphere, *2*(3), e00089-17.

Sugiyama, N., Nakagami, H., Mochida, K., Daudi, A., Tomita, M., Shirasu, K. (2008). Large-scale phosphorylation mapping reveals the extent of tyrosine phosphorylation in *Arabidopsis*. Molecular Systems Biology, *4*(193). https://doi.org/10.1038/msb.2008.32

Sun, J., Tian, C., Diamond, S., Glass, N. L. (2012). Deciphering transcriptional regulatory mechanisms associated with hemicellulose degradation in *Neurospora crassa*. Eukaryotic Cell, *11*(4), 482–493. https://doi.org/10.1128/EC.05327-11

Szklarczyk, D., Morris, J. H., Cook, H., Kuhn, M., Wyder, S., Simonovic, M., et al. (2017). The STRING database in 2017: Quality-controlled protein-protein association networks, made broadly accessible. Nucleic Acids Research, *45*, D362–D368. https://doi.org/10.1093/nar/gkw937

Tang, C.-T., Li, S., Long, C., Cha, J., Huang, G., Li, L., et al. (2009). Setting the pace of the Neurospora circadian clock by multiple independent FRQ phosphorylation events. PNAS, *106*(26), 10722–10727. https://doi.org/10.1073/pnas.0904898106

Tesmer, J. J. G. (2010). The Quest to Understand Heterotrimeric G Protein Signaling. Nat Struct Mol Biol, *17*(6), 650–652. https://doi.org/10.1038/nsmb0610-650.The

Thieme, N., Wu, V. W., Dietschmann, A., Salamov, A. A., Wang, M., Johnson, J., et al. (2017). The transcription factor PDR-1 is a multi-functional regulator and key component of pectin deconstruction and catabolism in *Neurospora crassa*. Biotechnology for Biofuels, *10*(1), 1–21. https://doi.org/10.1186/s13068-017-0807-z

Tian, C., Beeson, W. T., Iavarone, A. T., Sun, J., Marletta, M. A., Cate, J. H. D., Glass, N. L. (2009). Systems analysis of plant cell wall degradation by the model filamentous fungus *Neurospora crassa*. PNAS, *106*(52), 22157–22162. https://doi.org/10.1073/pnas.0906810106

Urano, D., Czarnecki, O., Wang, X., Jones, A. M., Chen, J. D., et al. (2015). *Arabidopsis* Receptor of Activated C Kinase1 Phosphorylation by WITH NO LYSINE8 KINASE 1. Plant Physiology, *167*(2), 507–516. https://doi.org/10.1104/pp.114.247460

van Munster, J. M., Daly, P., Delmas, S., Pullan, S. T., Blythe, M. J., Malla, S., et al. (2014).

1353 The role of carbon starvation in the induction of enzymes that degrade plant-derived
1354 carbohydrates in *Aspergillus niger*. Fungal Genetics and Biology, *72*, 34–47.
1355 https://doi.org/10.1016/j.fgb.2014.04.006
1356 Vinuselvi, P., Kim, M. K., Lee, S. K., Ghim, C. (2012). Rewiring carbon catabolite repression
1357 for microbial cell factory. BMB, *45*(2), 59–70.
1358 Vitalini, M. W., Paula, R. M. De, Goldsmith, C. S., Jones, C. A., Borkovich, K. A., Bell-
1359 pedersen, D. (2007). Circadian rhythmicity mediated by temporal regulation of the
1360 activity of p38 MAPK. PNAS, *104*(46), 18223–18228.
1361 Vogel, H. J. (1956). A Convenient Growth Medium for *Neurospora crassa*. Microbial
1362 Genetics Bulletin, *13*, 42–47.
1363 Vries, R. P. De, Jansen, J., Aguilar, G., Par, L., Joosten, V., Wu, F., et al. (2002). Expression
1364 profiling of pectinolytic genes from *Aspergillus niger*. FEBS Letters, *530*, 41–47.
1365 Wang, B., Kettenbach, A. N., Zhou, X., Loros, J. J., Dunlap, J. C. (2019). The Phospho-Code
1366 Determining Circadian Feedback Loop Closure and Output in *Neurospora*. Molecular
1367 Cell. https://doi.org/https://doi.org/10.1016/j.molcel.2019.03.003
1368 Wang, Z., An, N., Xu, W., Zhang, W., Meng, X., Chen, G., Liu, W. (2018). Functional
1369 characterization of the upstream components of the Hog1-like kinase cascade in
1370 hyperosmotic and carbon sensing in *Trichoderma reesei*. Biotechnology for Biofuels,
1371 11(1), 1–17. https://doi.org/10.1186/s13068-018-1098-8
1372 Wang, B., Li, J., Gao, J., Cai, P., Han, X., Tian, C. (2017). Identification and characterization
1373 of the glucose dual-affinity transport system in *Neurospora crassa*: Pleiotropic roles in
1374 nutrient transport, signaling, and carbon catabolite repression. Biotechnology for
1375 Biofuels, *10*(1), 1–22. https://doi.org/10.1186/s13068-017-0705-4
1376 Wang, B., Zhou, X., Loros, J. J., Dunlap, J. C. (2015). Alternative Use of DNA Binding
1377 Domains by the Neurospora White Collar Complex Dictates Circadian Regulation and
1378 Light Responses. Molecular and Cellular Biology, *36*(5), 781–793.
1379 https://doi.org/10.1128/mcb.00841-15
1380 Wart, V., Unit, P. (1993). On target with a new mechanism for the regulation of protein
1381 phosphorylation. Trends Biochem.Sci, (May), 172–177.
1382 Weirauch, M. T., Yang, A., Albu, M., Cote, A., Montenegro-, A., Drewe, P., et al. (2014).
1383 Determination and Inference of Eukaryotic Transcription Factor Sequence Specificity.
1384 Cell, *158*(6), 1431–1443. https://doi.org/10.1016/j.cell.2014.08.009.Determination
1385 Welchman, R. L., Gordon, C., Mayer, R. J. (2005). Ubiquitin and ubiquitin-like proteins as
1386 multifunctional signals. Nature Reviews Molecular Cell Biology, *6*(8), 599–609.

https://doi.org/10.1038/nrm1700

Whitmarsh, A. J., Davis, R. J. (2000). Regulation of transcription factor function by phosphorylation. Cellular and Molecular Life Sciences*: CMLS*, *57*, 1172–1183.

Willardson, B. M., Tracy, C. M. (2012). Chaperone-Mediated Assembly of G Protein Complexes. In D. J. Dupré, T. E. Hébert, & R. Jockers (Eds.), GPCR Signalling Complexes -- Synthesis, Assembly, Trafficking and Specificity (pp. 131–153). Dordrecht: Springer Netherlands. https://doi.org/10.1007/978-94-007-4765-4_8

Xiong, Y., Coradetti, S. T., Li, X., Gritsenko, M. A., Clauss, T., Petyuk, V., et al. (2014). The proteome and phosphoproteome of *Neurospora crassa* in response to cellulose, sucrose and carbon starvation. Fungal Genetics and Biology, *72*, 21–33. https://doi.org/10.1016/j.fgb.2014.05.005

Xiong, Y., Sun, J., Glass, N. L. (2014). VIB1 , a Link between Glucose Signaling and Carbon Catabolite Repression, Is Essential for Plant Cell Wall Degradation by *Neurospora crassa*. PLoS Genetics, *10*(8), e1004500. https://doi.org/10.1371/journal.pgen.1004500

Xiong, Y., Wu, V. W., Lubbe, A., Qin, L., Deng, S., Kennedy, M.,et al. (2017). A fungal transcription factor essential for starch degradation affects integration of carbon and nitrogen metabolism. PLos Genetics, *13*(5), e1006737.

Xue, Y., Batlle, M., Hirsch, J. P. (1998). GPR1 encodes a putative G protein-coupled receptor that associates with the Gpa2p GAlfa subunit and functions in a Ras□independent pathway. The EMBO Journal, *17*(7), 1996–2007. https://doi.org/10.1093/emboj/17.7.1996

Yang, Q., Poole, S. I., Borkovich, K. A. (2002). A G-Protein beta Subunit Required for Sexual and Vegetative Development and Maintenance of Normal G alpha Protein Levels in *Neurospora crassa*. Eukaryotic Cell, *1*(3), 378–390. https://doi.org/10.1128/EC.1.3.378

Zhang, X., Jain, R., Li, G. (2016). Roles of Rack1 Proteins in Fungal Pathogenesis. BioMed Research International, *2016*(4130376), 1–8. https://doi.org/10.1155/2016/4130376

Znameroski, E. A., Coradetti, S. T., Roche, C. M., Tsai, J. C., Iavarone, A. T., Cate, J. H. D., Glass, N. L. (2012). Induction of lignocellulose-degrading enzymes in *Neurospora crassa* by cellodextrins. PNAS, *109*(16), 6012 LP-6017. https://doi.org/10.1073/pnas.1118440109

Figure 1: Proteome and phospho-proteome classification. A) Phospho-peptide distribution according to substrates. For this analysis, only the specific phospho-peptides (AScore >13, P<0.05) were considered. B) Functional classification of proteins with specific phospho-peptides for each condition. Substrate abbreviations: GalAR, D-GalA+L-Rha; D-Glc, D-Glucose; D-Xyl, D-Xylose; Cel, cellobiose; Gm, Glucomannodextrins; NC, no carbon.

Figure 2: Protein-Protein Interaction network. A) The PPI network of all proteins identified by proteomics and phospho-proteomics in our experiments. Functional categories related to signaling are color-coded: green, signal transduction; orange, kinases; blue, metabolism; pink, transcription factors; red, transporters. B) Visualization of proteins in the PPI with specific phospho-peptides (independent of AScores) found in each experimental condition. Squares represent phosphorylated proteins, circles non-phosphorylated proteins. Red border-colored squares represent proteins phosphorylated specifically at the displayed condition and when filled, the proteins belong to one of the functional categories described in (A). GalAR (D-GalA+L-Rha), D-Glc (D-Glucose), D-Xyl (D-Xylose), Cel (cellobiose), Gm (Glucomannodextrins), NC (No carbon).

Figure 3: Carbon source-dependent changes of CR-1 interactions. A) Phospho-site distribution of CR-1 in response to substrate conditions. Picture shows all possible sites of phosphorylation. GalAR (D-GalA+L-Rha), D-Glc (D-Glucose), D-Xyl (D-Xylose), Cel (cellobiose), Gm (Glucomannodextrins), NC (No carbon). Colored circles represent sites with Ascore > 13, and grey circles with AScore < 13. B) Set of proteins directly interacting with CR-1. Colors according to functional categories: green, signal transduction; orange, kinases; blue, metabolism. C) Sub-PPI-networks of CR-1 nodes represent proteins that interact with CR-1, those peptides were found phosphorylated at specific condition. Colors according to functional categories described in (B). D) Mycelial biomass (dry weight) of the Δ*cr-1* mutant relative to on D-Glc, xylan, arabinan, glucomannan and pectin. Error bars represent the standard deviation from triplicate experiments. Statistical differences were calculated using *t*-test (***: p<10E-5).

Figure 4: F-Box screening. A) Growth phenotypes of the F-box mutants on glucose (D-Glc), xylan, arabinan, glucomannan and pectin. B) The mutant strains were grown on 1% xylose (D-Xyl) plates. 2-DG resistance: deletion strains were grown on 2% D-Xyl as control and 2% D-Xyl + 0.2% 2-DG. Allyl alcohol (AA)–sensitivity: deletion strains were grown on 1% D-Glc

as control and 1% D-Glc + 100 mM AA. C) Xylanase activities of F-box deletion strains of *N. crassa* and *A. nidulans*. Error bars represent standard deviation from triplicate experiments. Statistical differences were calculated between the mutants and WT within each treatment using *t*-test (*: $p<0.05$, **: $p<0.001$).

1459

1460 Table 1: Summary of discussed classes of genes, with the respective protein name. The
1461 numbers of identified phospho-peptides correspond to all variant phospho-peptides identified
1462 experimentally. The number of phosphorylation sites correspond to the unambiguous
1463 identification of S, Y and T (Ascore > 13).

1464

Function	Gene ID	Protein name *	Number of identified phospho-peptides	Number of phosphosites
Transcription factors	NCU09068	NIT-2	84	18
	NCU10346	ADA-13	43	14
	NCU09315	NCU-1	23	9
	NCU01345	ASL-1	20	6
	NCU03725	VIB-1	20	10
	NCU08807	CRE-1	15	6
	NCU07788	COL-26/BglR	6	4
	NCU07705	CLR-1	2	2
	NCU05846	CLR-3	3	3
G-protein	NCU00440	GNB-1	2	1
	NCU05810	CPC-2	1	1
	NCU00441	PhLP1	3	4
	NCU03238	GPR-9	1	1
	NCU03253	GPR-8	12	5
	NCU04106	GPR-17	5	2
	NCU04931	GPR-18	1	1
	NCU04987	GPR-10	6	3
	NCU06987	GPR-14	1	1
	NCU08718	GPR-35	1	1
	NCU09195	GPR-6	3	3
	NCU09201	GPR-37	2	2
	NCU09427	GPR-3	1	1
F-Box	NCU01081	hp/pc	1	1
	NCU01216	HPTH-1	1	1
	NCU03658	SPP-1/Fbx-9	1	1
	NCU03881	hp	3	1
	NCU04540	FWD-1	4	2
	NCU05939	CDC4/Fbx-22	7	6
	NCU06250	pc/Fbx-20	1	1
	NCU06483	pc	1	1
Two-component regulatory systems- HHs	NCU00939	DCC-1	16	6
	NCU01823	pc	16	11
	NCU01833	NIK-2	3	1
	NCU02057	pc	3	2
	NCU02815	OS-1	2	1
	NCU03164	pc	3	3
	NCU04615	SLN1	3	2
	NCU07221	HCP-1	9	6
	NCU01895	RRG-1	3	3
	NCU02413	RRG-2	3	2
	NCU07378	STK-12	26	10
Serine/Threonine protein Kinase	NCU02556	HAT-2	1	1
	NCU00108	STK-13	1	1
	NCU06685	STK-47	1	1
	NCU06230	STK-39	1	1
	NCU05608	TOR	9	4
	NCU03200	STK-10	62	22
	NCU07872	PRK-2/YAK1	23	13
	NCU06240	PKAc-1	39	3
	NCU00682	PKAc-2	2	1
Signaling crosstalk carbon sensing-light respons- circadian rhythmicity	NCU02265	FRQ	14	12
	NCU02356	WC-1	8	5
	NCU00902	WC-2	2	1
	NCU03363	FRH	2	1
	NCU01154	SUB-1	4	3
	NCU01731	VE-1	9	3
MAP kinase pathways	NCU00587	PBS2/OS-5	7	5
	NCU07024	HOG1/OS-2	5	2
	NCU06182	NRC-1	10	8

	NCU06688	pc	13	8
	NCU07425	pc	7	5
	NCU07521	FWD-2	3	3
	NCU07746	pc	4	1
	NCU07996	pc	2	1
	NCU08563	SCON-2	5	2
	NCU08642	pc/Fbx-19	5	2
	NCU09807	hp/pc	6	4
Casein-kinases	NCU05485	CKB1	9	7
	NCU00685	CK-1A	5	3

	NCU04612	MEK-2	11	6
	NCU02393	MAK-2	3	2
	NCU02234	MIK-1	27	13
	NCU06419	MEK-1	19	8
	NCU09842	MAK-1	8	3
	NCU03071	OS-4	17	6
cAMP signaling pathway	NCU08377	CR-1	31	18
	NCU01166	MCB	10	4
	NCU06240	PKAC-1	39	8
	NCU00682	PKAC-2	2	1
	NCU00478	ACON-2	9	5

*pc- protein coding / * hp- hypothetical protein

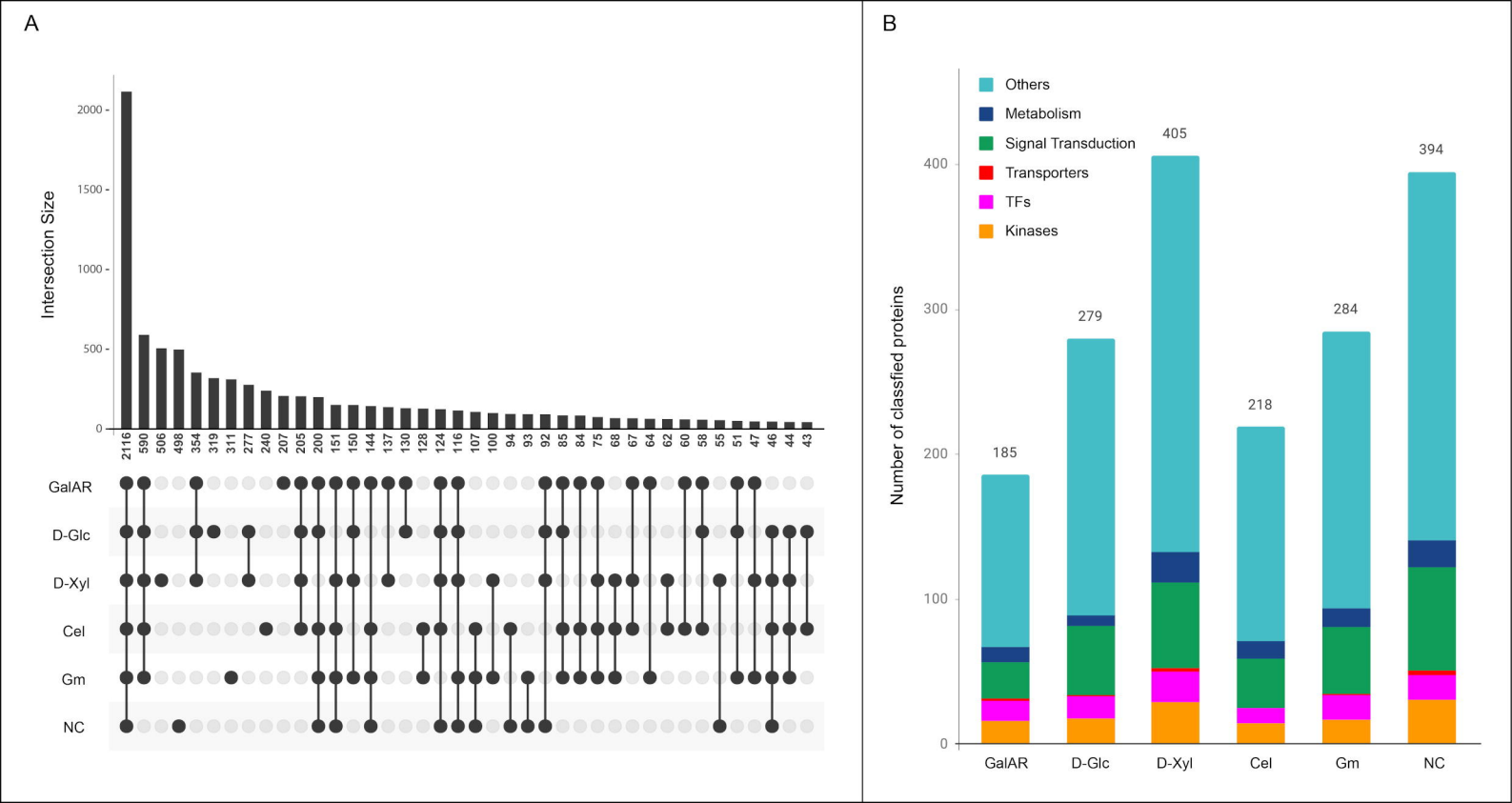
A
Intersection Size
2000
1500
1000
500
0
2116 590 506 498 354 319 311 277 240 207 205 200 151 150 144 137 130 128 124 116 107 100 94 93 92 85 84 75 68 67 64 62 60 58 55 51 47 46 44 43
GalAR
D-Glc
D-Xyl
Cel
Gm
NC
B
Others
Metabolism
Signal Transduction
Transporters
TFs
Kinases
Number of classfied proteins
400
300
200
100
0
185
279
405
218
284
394
GalAR
D-Glc
D-Xyl
Cel
Gm
NC

A

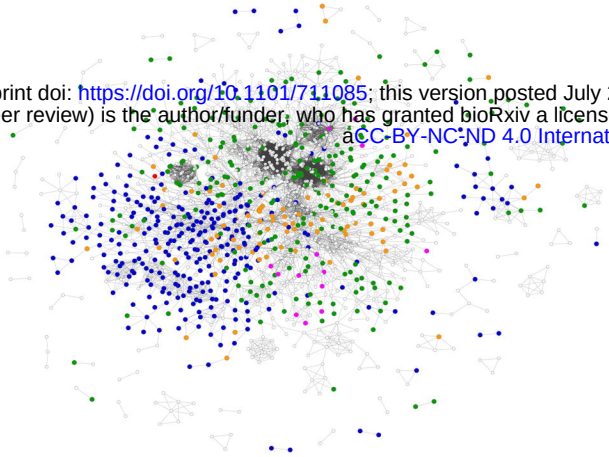

Kinase
Metabolism
Transporter
Transcription Factor
Signal Transduction

B

GalAR

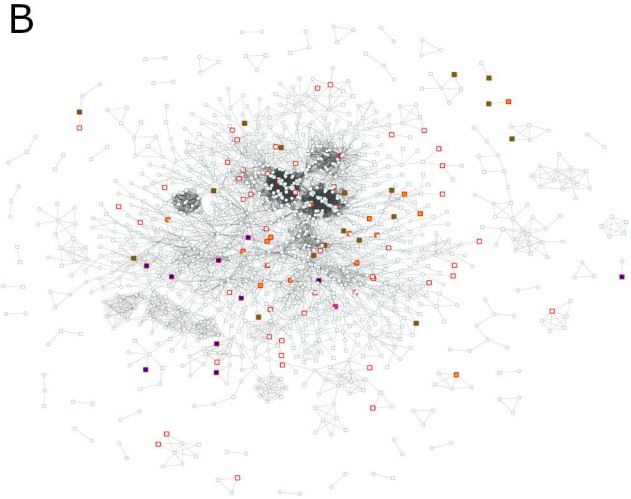

D-Xyl

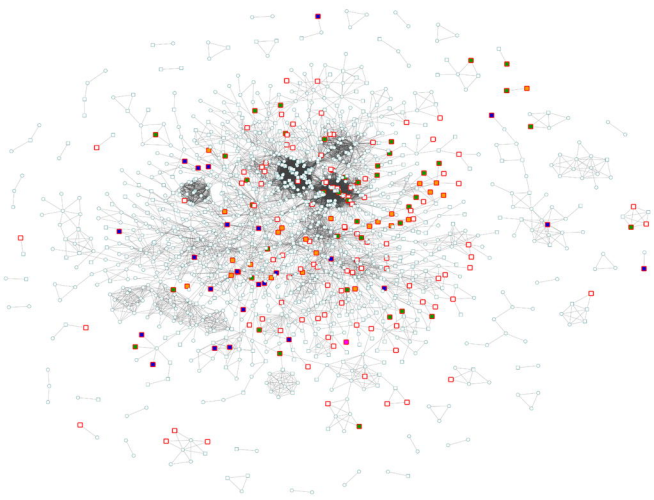

D-Glc

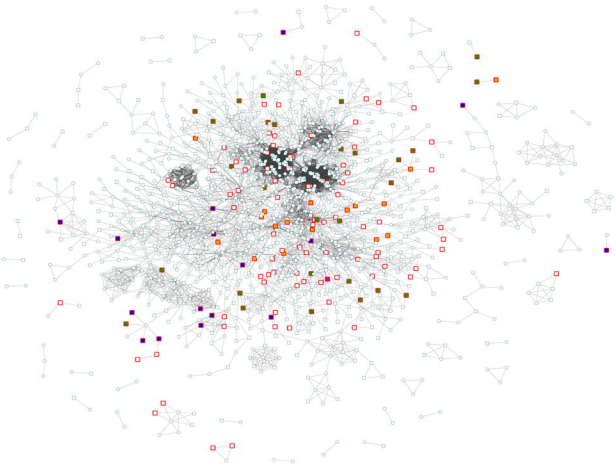

Cel

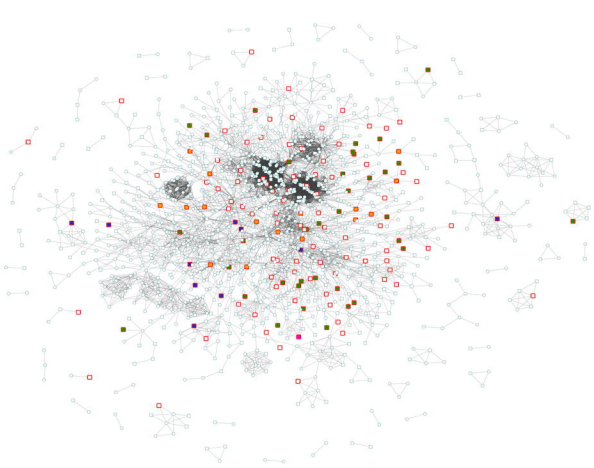

Gm

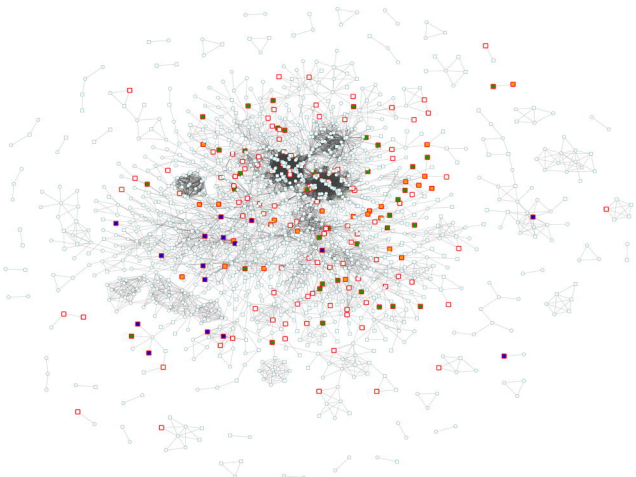

NC

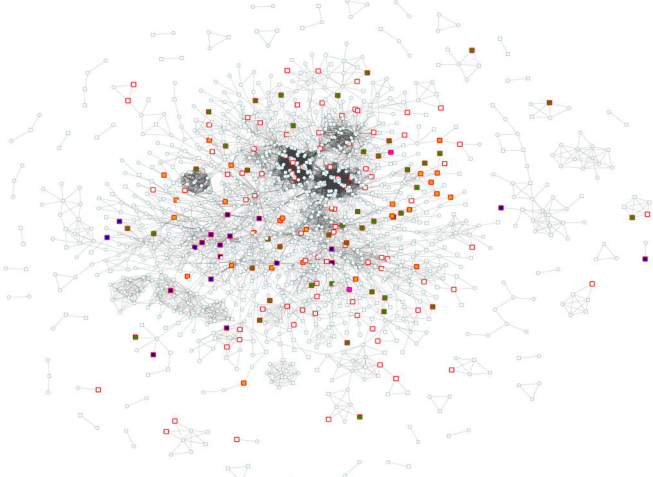

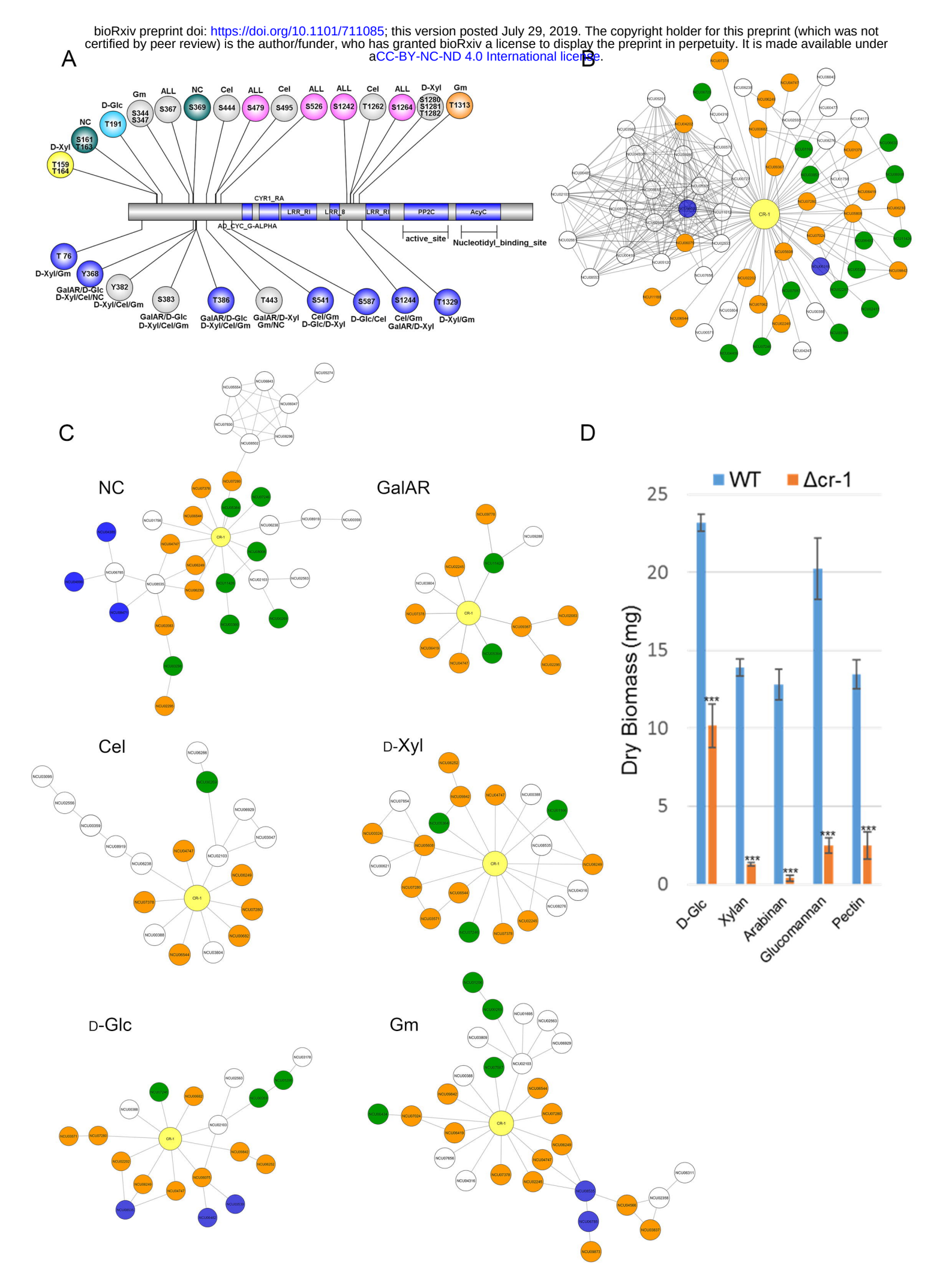

A

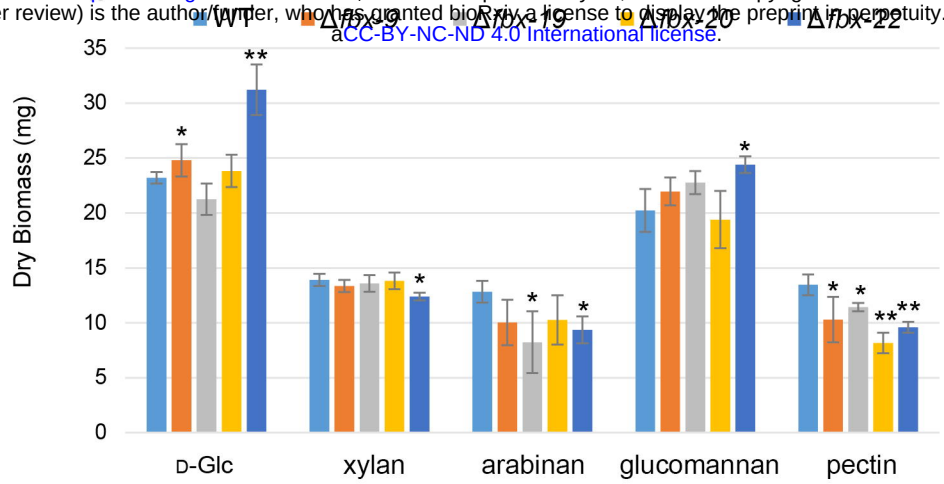

B

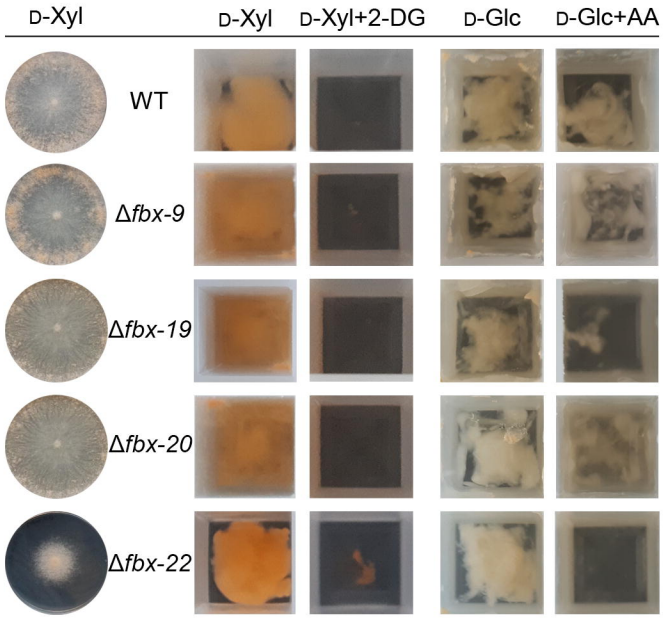

C